

**FEASIBILITY OF SUPERCRITICAL CARBON DIOXIDE
AS A DRILLING FLUID FOR DEEP UNDERBALANCED
DRILLING OPERATIONS**

A Thesis

**Submitted to the Graduate Faculty of the
Louisiana State University and
Agricultural and Mechanical College
in partial fulfillment of the
requirements for the degree of
Master of Science in Petroleum Engineering**

in

The Craft and Hawkins Department of Petroleum Engineering

**by
Anamika Gupta
B.E., Mumbai University Institute of Chemical Technology, 2003
May 2006**

ACKNOWLEDGEMENTS

I would like to express my gratitude to my advisor, Dr. Anuj Gupta, for his constant guidance and support. He has always been extremely supportive and shared the enthusiasm of working on an interesting project like this. My special thanks to my examining committee members, Professor Julius Langlinais and Professor John Smith for their suggestions and co-operation. Their experience and wisdom helped this project immensely. I am grateful to the Craft and Hawkins Department for giving me the opportunity to learn. I would like to thank my parents and family for their encouragement and blessings. I would like to extend a special acknowledgement for Samarth who has always been there to bring out the best in me. I am extremely grateful to Dr. P.V.Suryanarayana, Dr. Ravi Vaidya and my colleagues at Blade Energy Partners for their support in the completion of my thesis and the opportunity to learn at Blade. All my friends at LSU and elsewhere have been extremely generous and I would like to thank them all.

TABLE OF CONTENTS

ACKNOWLEDGEMENTS.....	ii
LIST OF TABLES.....	v
LIST OF FIGURES.....	vi
ABSTRACT.....	viii
CHAPTER 1. INTRODUCTION.....	1
1.1 Example Case Study.....	1
1.2 Properties of Supercritical Carbon Dioxide.....	2
1.3 Proposed Solution.....	4
CHAPTER 2. LITERATURE SURVEY.....	6
2.1 Sources of CO ₂	6
2.2 Underbalanced Drilling (UBD).....	7
2.3 Coiled Tubing Underbalanced Drilling (CTUBD).....	10
2.4 Previous Work on Drilling with SCCO ₂ by Kolle[13].....	11
CHAPTER 3. MODEL DEVELOPMENT.....	13
3.1 PVT Model.....	13
3.2 Heat Transfer Model.....	17
3.3 Circulation Model.....	17
3.4 Assumptions of the Model.....	19
3.5 Methodology.....	19
CHAPTER 4. CASE STUDY APPLICATION.....	21
4.1 Operations Summary.....	21
4.2 Input Data [1].....	21
4.3 Simulation Results and Discussions.....	23
CHAPTER 5. WELLFLO 7 MODELING AND RESULTS.....	29
5.1 About WellFlo 7.....	29
5.2 Comparison of Results from Proposed Model and WellFlo 7.....	30
CHAPTER 6. CORROSION PROBLEMS WITH CO₂ AND ITS CUTTINGS CARRYING CAPACITY.....	38
6.1 Corrosion Potential of CO ₂	38
6.2 Low Viscosity of CO ₂ : Potential for Using Thickening Agents.....	42
CHAPTER 7. QUALITATIVE ANALYSIS OF DRILLING WITH SUPERCRITICAL CO₂.....	45
7.1 Potential Advantages.....	45
7.2 Possible Problems.....	45

7.3 Economic Considerations.....	47
CHAPTER 8. CONCLUSIONS AND RECOMMENDATIONS.....	49
8.1 Conclusions.....	49
8.2 Recommendations.....	50
REFERENCES.....	51
APPENDIX A: PROPERTIES OF CARBON DIOXIDE.....	54
APPENDIX B: SPREADSHEET AND VB CODE EXAMPLE.....	56
APPENDIX C: HEAT TRANSFER MODEL BASED ON THE WORK OF HOLMES AND SWIFT [18].....	60
VITA.....	63

LIST OF TABLES

1. Chung et al. Coefficients to Calculate $E_i = a_i + b_i \omega$ [14].....	17
2. Input Parameters for the Model for BHP = 400 psi.....	23
3. Spreadsheet Output for Calculations on the Annulus Side.....	59

LIST OF FIGURES

1. Phase Diagram of Carbon Dioxide[2].....	3
2. Phase Change of Carbon Dioxide to Supercritical State[3].....	3
3. Hydrate Formation Regions of Gases[4].....	4
4. Example of a Finite Element Considered in the Model.....	20
5. Flowchart of the Proposed Model.....	20
6. Wellbore Schematic for Example Case Study.....	22
7. Variation of Density of CO ₂ with Pressure at Different Temperature Values.....	24
8. Variation of Viscosity of CO ₂ with Temperature at Different Pressure Values.....	25
9. Variation of CO ₂ Density with Depth.....	26
10. Variation of Circulating Pressure with Depth.....	26
11. Variation of Bottom-hole Pressure with Choke Pressure.....	27
12. CTR Variations with Depth and Cuttings Size.....	28
13. Circulating Pressure Profile of Foam of Nitrogen and Water.....	31
14. Cuttings Transport Ratios for 0.1” and 0.2” Cuttings for Foam.....	32
15. Comparison of Circulating Pressure Profile from Model and WellFlo 7.....	33
16. Comparison of Frictional Pressure Drop with Choke Pressure from Model and WellFlo 7	34
17. Comparison of Frictional Pressure Drop with Gas Flow Rate from Model and WellFlo 7	34
18. Comparison of Density Predictions from Model and WellFlo 7.....	35
19. CO ₂ Density Variations in the Tubing and the Annulus.....	36
20. CTR Variations with Depth for Different Sized Cuttings Using WellFlo 7.....	37
21. de Waard and Milliams Nomogram[16].....	39

22. Corrosion Rates Along the Annulus Length for Different Choke Pressures.....	41
23. SEM Images of Foam Produced from CO ₂ -gels.....	44
C1. Temperature Profile of CO ₂ in the Tubing and Annulus.....	62

ABSTRACT

Feasibility of drilling with supercritical carbon dioxide to serve the needs of deep underbalanced drilling operations has been analyzed. A case study involving underbalanced drilling to access a depleted gas reservoir is used to illustrate the need for such a research. For this well, nitrogen was initially considered as the drilling fluid. Dry nitrogen, due to its low density, was unable to generate sufficient torque in the downhole motor. The mixture of nitrogen and water, stabilized as foam generated sufficient torque but made it difficult to maintain underbalanced conditions. This diminished the intended benefit of using nitrogen as the drilling fluid.

CO₂ is expected to be supercritical at downhole pressure and temperature conditions, with density similar to that of a liquid and viscosity comparable to a gas. A computational model was developed to calculate the variation of density and viscosity in the tubing and the annulus with pressure, temperature and depth. A circulation model was developed to calculate the frictional pressure losses in the tubing and the annulus, and important parameters such as the jet impact force and the cuttings transport ratio. An attempt was made to model the temperatures in the well using an analytical model. Corrosion aspects of a CO₂ based drilling system are critical and were addressed in this study.

The results show that the unique properties of CO₂, which is supercritical in the tubing and changes to vapor phase in the annulus, are advantageous in its role as a drilling fluid. It has the necessary density in the tubing to turn the downhole motor and the necessary density and viscosity to maintain underbalanced conditions in the annulus. The role of a surface choke is crucial in controlling the annular pressures for this system. A carefully

designed corrosion control program is essential for such a system. Results of this study may also be important for understanding the flow behavior of CO₂ in CO₂ sequestration and CO₂ based enhanced oil recovery operations.

CHAPTER 1

INTRODUCTION

Supercritical carbon dioxide (SCCO₂) has attracted the attention of researchers because of its unique properties attainable for some drilling applications. The present work addresses the potential advantages and feasibility of using SCCO₂ as a drilling fluid in underbalanced drilling of depleted/ sub-normal pressure formations. A potential application where the use of supercritical CO₂ as a drilling fluid may be of great value is highlighted by the following case study.

1.1. Example Case Study

This refers to a depleted gas well in the Darbun field in Mississippi, where depletion of the reservoir over time had led to an extremely low pressure of 700 psi at a depth of 14,340 feet. It is believed that the casing had collapsed due to such an extreme pressure imbalance [1]. In order to regain production from this depleted gas reservoir, the operator decided to drill a sidetracked well branch, from the existing completed well. After the sidetrack operation, conventional drilling through the depleted sixty feet thick reservoir section was unacceptable. It would have caused lost circulation problems and differential sticking due to excessive overbalance resulting from the large hydrostatic pressure exerted by a tall column of mud. This could also cause severe reduction in productivity due to potential water-blockage and formation damage.

To overcome these problems, it was decided to drill the depleted zone with nitrogen as a drilling fluid, in order to maintain wellbore pressure below the reservoir pressure while drilling. Coiled tubing drilling (CTD) was the selected method as it provided pressure

control while tripping and allowed continuous operation without the time consuming tripping operation for making connections as is done for conventional drillpipe.

Unforeseen operational problems developed while drilling the target reservoir section with pure nitrogen. Low density of nitrogen did not allow generation of sufficient torque to turn the downhole motor and the drill-bit. To overcome this problem, it was decided to drill with foam of nitrogen and water to address the motor torque problem. Though the motor was efficiently powered by the foam, the increased frictional losses and hydrostatic pressure exerted, due to the addition of water, made it difficult to maintain the desired underbalanced conditions in the annulus.

CO₂ is known to have unique properties in the supercritical phase and this case study offered an opportunity to investigate its utility as a drilling fluid.

1.2. Properties of Supercritical Carbon Dioxide

A substance above its critical temperature and critical pressure is considered to be a supercritical fluid. The critical point represents the highest temperature and pressure at which the vapor and liquid phase of a substance can co-exist in equilibrium. Above the critical point, the distinction between gas and liquid does not apply and the substance can only be described as a fluid. The physical properties of supercritical CO₂, such as, density, viscosity and diffusivity coefficient can be varied between limits of gas and near-liquid properties by controlling temperature and pressure. Since their physical properties can be adjusted to suit the desired application, they prove to be very useful. The properties of CO₂ are listed in Appendix A.

The phase diagram of carbon dioxide is shown in Figure 1 [2]. CO₂ is a supercritical fluid above 88 deg. F and 1074 psi.

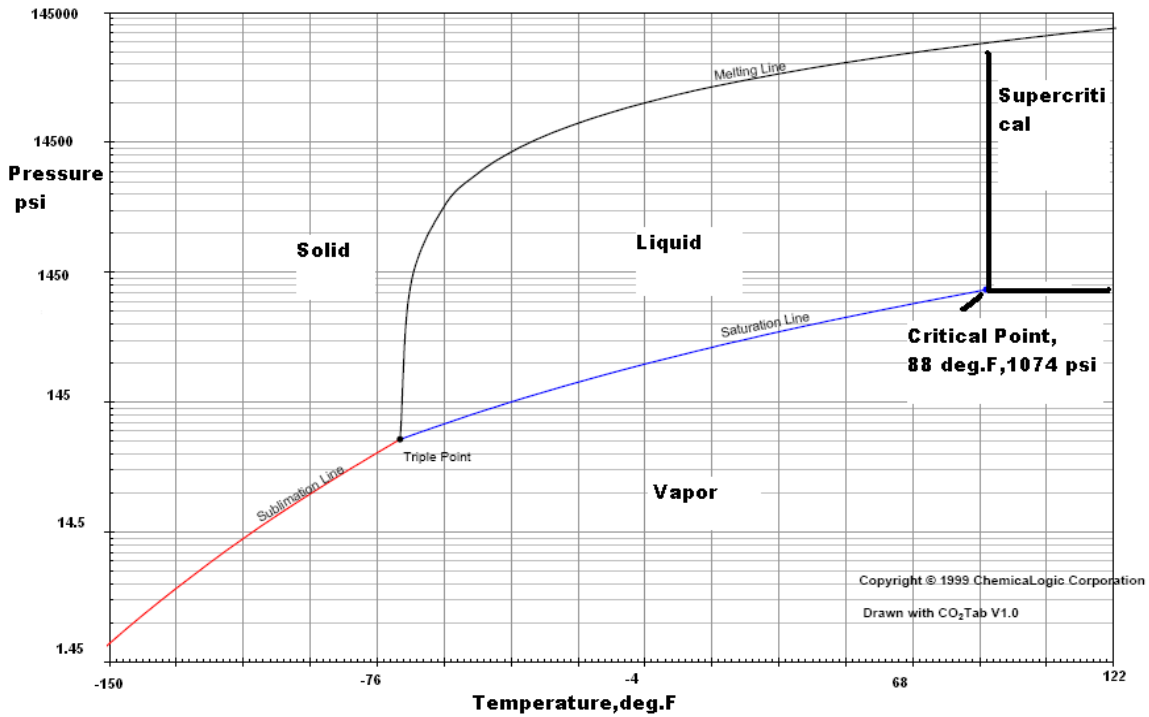


Figure 1. Phase Diagram of Carbon Dioxide [2]

Figure 2 illustrates the phase change of CO₂ from distinct gas and liquid phases to a homogeneous supercritical phase [3]. At supercritical conditions, CO₂ has a density similar to a liquid and viscosity and diffusivity comparable to a gas.

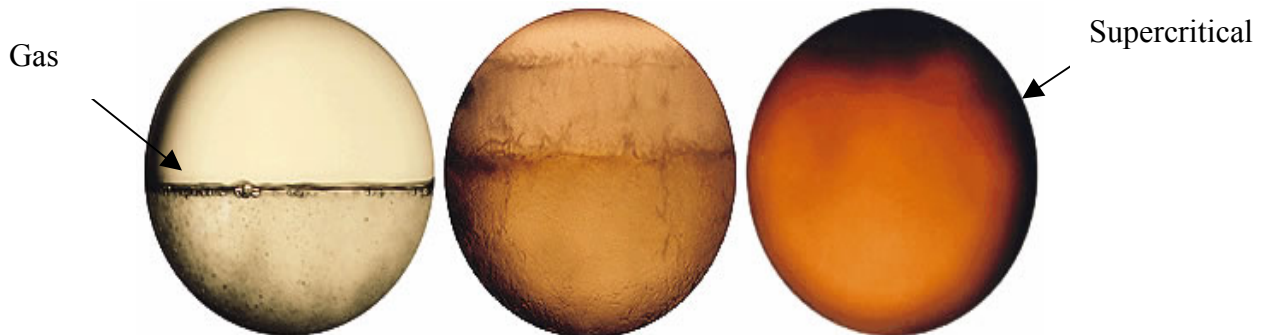


Figure 2. Phase Change of Carbon Dioxide to Supercritical State [3]

CO₂ is known to form hydrates and for safe operation of a system using CO₂, the operating pressures and temperatures must be selected to eliminate the possibility of hydrate formation. Hydrates are formed when gas molecules are trapped inside an ice like structure, typically at low temperature and high pressure conditions. Figure 3 illustrates the hydrate formation conditions for CO₂ which occur at temperature below 10 °C (50 °F) and pressure above 5 MPa (650 psi) [4].

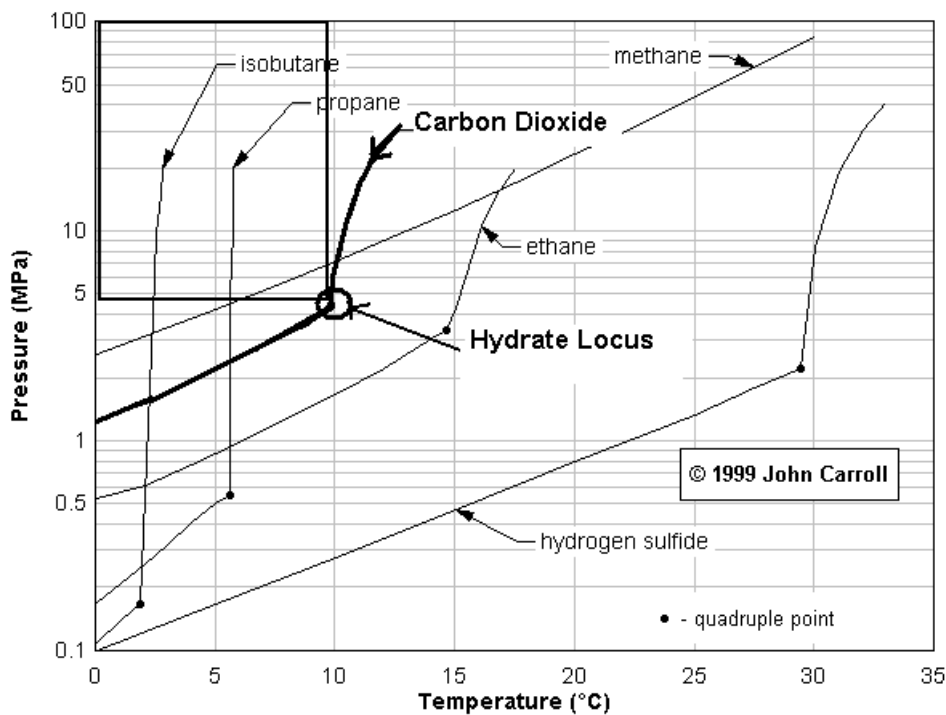


Figure 3. Hydrate Formation Regions of Gases [4]

1.3. Proposed Solution

The properties that CO₂ develops in the supercritical phase and the ability to tune the temperatures and pressures to bring the necessary phase changes, is the reason that it is being investigated as a potential solution to the problem described in the example case study. The aim is to inject CO₂ such that the dense phases that occur in the tubing run the downhole motor and later force a phase change across the nozzle in order to have the

lighter phase in the annulus to maintain the desired underbalance. Feasibility of such a system will be studied by developing a model that computes the change in properties with temperature and pressure, in addition to pressure losses as CO₂ is circulated through the coiled tubing system.

CHAPTER 2

LITERATURE SURVEY

The decision to investigate the use of supercritical CO₂ as a drilling fluid for the example case study was made after a thorough literature search. The availability of CO₂ from sources other than CO₂ natural reservoirs was looked into as many industrial processes produce CO₂ and could be potential sources. The benefits and drawbacks of under-balanced drilling with a coiled tubing drilling system were examined. The experimental work by Kolle [13] on jet-assisted drilling with supercritical CO₂ proved the potential of CO₂ as a jetting fluid for drilling applications and has been discussed in this chapter.

2.1. Sources of CO₂

The sources of CO₂ include natural CO₂ reservoirs, industrial sources and produced gas streams. Nearly all CO₂ enhanced oil recovery (EOR) projects in USA use CO₂ produced from reservoirs containing nearly pure CO₂ [5]. The price of CO₂ varies depending on the proximity of the CO₂ production wells [6]. Industrial sources such as natural gas processing, hydrogen production facilities and power plants, offer alternatives to naturally occurring CO₂, although more expensive ones. In addition to the cost of CO₂, there are other costs associated with its transport, compression and storage.

Drilling using SCCO₂ is a technology that is yet to be applied on a large scale in any field. However the major application of CO₂ in the petroleum industry has been in the EOR projects. The number of CO₂ EOR projects has remained steady or increased slightly with CO₂ production volumes increasing significantly [7]. The industry is now focusing on capturing CO₂ from industrial sources to reduce the dependence on natural occurring reservoirs and also to reduce CO₂ emissions in the atmosphere.

2.2. Underbalanced Drilling (UBD)

UBD is performed with drilling fluids that enable the borehole pressure to remain less than the formation pressure. The bottomhole circulating pressure is intentionally set to be less than the reservoir pressure. Due to this, the formation fluids enter the wellbore while drilling. In the case of UBD, the parameters for selecting the appropriate drilling fluid are different from the overbalanced drilling operation. For instance, for the case study being investigated, the drilling fluid must offer suitable hydraulic energy to run the downhole drilling motor. At the same time it should be able to carry the cuttings to the surface to get a good rate of penetration (ROP). Very importantly, it must be non-damaging.

The low density drilling fluids utilized to generate the underbalanced condition for a low-pressure reservoir include air, dry gases, mist, foam, and gasified liquids. In the example case study, the initial plan was to drill only with nitrogen, as the reservoir pressure was very low. The plan was then changed to drill with foam of water and nitrogen since pure nitrogen could not impart sufficient hydraulic energy to run the motor. Foams are a popular choice in UBD applications, primarily due to their excellent cuttings carrying capacity in comparison to gases. Beyer et al. [8] discuss, in detail, the flow behavior of foam as a well circulating fluid.

There are several papers [9, 10] where advantages of UBD have been discussed. Bennion et al. [9] present the praises and perils associated with UBD. The advantages of UBD presented by the authors include the following:

1. Reduction in invasive formation damage

Invasive damage is an important consideration for many formations, particularly in conventional drilling operations. It causes considerable reduction in the

productivity of a well. It may be caused by the physical migration of fines and clays due to fluid leakoff. Adverse reaction between invaded filtrate and formation or in-situ fluids (emulsions, precipitates and scales) also causes damage.

2. Increased rate of penetration (ROP)

Due to decreased pressure at the bit head, UBD operations demonstrate superior penetration rates in comparison to conventional drilling techniques.

3. Rapid indication of productive reservoir zones

As drilling is accompanied by production, proper flow monitoring of the produced fluids at surface can provide a good indication of productive zones of the reservoir.

4. Ability to flow /test well while drilling

The ability to conduct single or multirate drawdown tests while drilling proves beneficial to the operator, as the tests indicate the productive capacity of the formation and formation properties.

In addition to these, there are advantages associated with reduction of differential sticking and lost circulation problems.

Suryanarayana et al. [10] classify the benefits of UBD into two classes:

- **Cost Avoidance**

This includes mitigation of conventional drilling problems such as differential sticking and lost circulation. One also avoids costs associated with stimulation.

- **Value Creation**

This includes productivity improvement, increase in ultimate recovery and real-

time reservoir characterization while drilling. This is primarily due to the fact that UBD reduces or eliminates formation damage.

UBD is not a panacea for all drilling related problems. The right candidate selection is a must for it to be successful. Bennion et al. [9] also discuss the disadvantages associated with UBD which include:

a. Expense

UBD is usually more expensive than an overbalanced drilling operation, particularly in sour and offshore environments. However, these costs may be offset by improved productivity and increased ROP.

b. Safety concerns

As the well may be flowing while drilling there are some safety concerns. There are corrosion and flammability issues, especially when drilling with air or processed flue gas. Recent developments in surface equipment and CTD have helped to increase the reliability of UBD operations.

c. Wellbore stability concerns

This is particularly a concern for poorly consolidated and highly depleted formations. A reservoir by reservoir evaluation is required to quantify stability concerns for each UBD application.

d. Failure to maintain a continuously underbalanced condition during drilling and completion and resulting formation damage

Because there is no filter cake formed in UBD, the protective ability and presence of this filter cake as a barrier to fluid and solids invasion is not present if well experiences occasional overbalance.

e. Overbalanced/conventional completion kill jobs

This negates the benefit of using UBD. To obtain maximum benefit to well productivity, underbalanced completion procedures must be used.

f. Spontaneous imbibition and counter-current imbibition effects

Adverse capillary effects can result in imbibition of fluids in near-wellbore region which could reduce the permeability or flow capacity due to the incompatibility of formation (or connate fluid) with the imbibed fluid. Thus a very good understanding of formation wettability coupled with base fluid selection for UBD is important.

g. Difficulty in zones of extreme permeability

Extremely high permeability formation can result in risks associated with handling huge volumes of produced fluids and high pressures on the surface equipment. Improvement in surface handling equipment is needed.

To summarize, there are risks associated with UBD. Screening tests using criteria for the right candidate selection must be conducted along with careful reservoir characterization. If rigorous well engineering procedures are followed, significant economic and technical benefits can be achieved.

2.3. Coiled Tubing Underbalanced Drilling (CTUBD)

Coiled tubing (CT) refers to a continuous reel of pipe wound on a spool at the surface. Depending on the diameter of the pipe and the spool size, the length of the CT varies. Scherchel et al. [11] discuss the CT technology being applied to underbalanced drilling operations. According to the authors, CT systems are quite relevant for drilling underbalanced. The primary advantage is the ability to control pressure while tripping.

This allows minimal pipe handling and faster trip times. The continuous nature (no connections) of the coiled tubing string facilitates maintenance of a constant bottomhole pressure with no forced surging of the reservoir. The rig footprint is small and set-up is quicker. As the CT is not rotated, mechanical damage (pasting of cuttings over borehole wall) is avoided. Scherchel et al. discuss, in details, the equipment for the CTUBD operation. The bottomhole assembly (BHA) can be electrically connected to the surface with wireline, which allows transmission of steering tool data to the surface. Electrical functionality of the BHA includes MWD capabilities, acquisition of pressure, temperature, BHA vibration data, all measured in real time. The drill motor is attached directly beneath the orienter and is the only part of the BHA which rotates while drilling.

If the reservoir has been determined to be a UBD candidate, then coiled tubing's mechanical and hydraulic limitations to the drillable lengths should be evaluated. In addition, there are fatigue limitations associated with CT due to bending and straightening of the CT at the surface. UBD generally involves circulating two phase fluid system and the volumetric flow rate through the motor is variable, dependent on the bottomhole circulating pressure. Thatcher et al. [12] present the planning and execution of the integrated service of CT and UBD through a case history.

2.4. Previous Work on Drilling with SCCO₂ by Kolle [13]

Kolle [13] has reported pioneering work in the field of jet-assisted CTD with SCCO₂. The goal of ultra-high pressure (UHP), jet-assisted drilling is to increase the rate of penetration (ROP) in deeper oil and gas wells, where the rocks become harder and more difficult to drill using conventional drill bits. The ultrahigh pressure, high velocity jet cuts a small kerf in the bottom of the borehole that enhances the mechanical drilling action of

the conventional bit. Jet erosion is an order of magnitude less efficient than mechanical drilling. Despite this inefficiency, jet drilling is attractive for small diameter holes because the jet hydraulic power is much higher than the mechanical power available from small diameter motors. CT is an attractive option for jet-assisted drilling as it allows for continuous circulation of low-solids drilling fluids. However, the bending fatigue is compounded by internal pressure and tubing tension.

Experiments reported by Kolle [13] using water and SCCO₂ indicate that SCCO₂ can cut hard shale, marble and granite at much lower pressure than water. This demonstrates that SCCO₂ can provide better jet-erosion and mechanical drilling rates than water based-fluids. Small-scale pressure drilling tests were reported for shale with SCCO₂ using a microbit with a drag cutter [13]. The rate of penetration in Mancos shale with CO₂ was 3.3 times that with water.

The drilling system described by Kolle [13] involves injecting liquid CO₂ in the CT using a high-pressure plunger pump. It becomes supercritical as it enters the tubing and powers the downhole motor. After exiting the nozzle, a phase change occurs in the annulus from supercritical to the gas phase. The drill motor used is a high-pressure vane motor that can be run by dry gas including high-pressure SCCO₂. The surface choke provides the necessary control of the bottomhole pressure.

The model for the proposed system is based on calculating the pressure losses in tubing, borehole pressure and pressures in the annulus assuming turbulent Newtonian flow. The density and viscosity data is modeled using Peng Robinson equation of state. From the production enhancement perspective, SCCO₂ is a non-damaging fluid that is known to stimulate production with immediate payback to the operator [13].

CHAPTER 3

MODEL DEVELOPMENT

Designing a successful system that utilizes supercritical CO₂ as a drilling fluid requires accurate modeling and prediction of the phase behavior of CO₂ as it traverses down the tubing, expands across the bit-nozzles and returns up the annulus. The required model is developed as a Visual-Basic-Excel® program that allows the user to perform sensitivity analysis using a spreadsheet. The algorithm is coded in macros written in Visual Basic and can be run using Microsoft Excel®. The iterations for convergence are done using the Solver add-in application in Excel®. The model consists of three key components:

- PVT Model
- Heat Transfer Model
- Circulation Model

3.1. PVT Model

An understanding of the phase behavior of CO₂ is essential for its use as a drilling fluid. Properties of importance such as density, viscosity and compressibility of CO₂ are no longer constant and their variation with depth is calculated using the PVT model.

The Peng Robinson equation of state [14] is used to calculate the density for each pressure and temperature combination. Carroll and Boyle [15] compared several methods (Soave-Kwong-Redlich (SRK), Peng Robinson (PR) and Patel-Teja (PT)) for calculating gas densities for acid gas injection applications. Their work spanned temperature from 32 °F to 302 °F and pressures from atmospheric to 4351 psi. They concluded that PR is more accurate in predicting densities of pure components.

The Peng Robinson Equation of state is represented by equation 2,

$$P = \frac{RT}{mV - b} - \frac{a(T)}{mV(mV + b) + b(mV - b)} \quad (2)$$

where,

P = Pressure, Pa,

T = Temperature, K,

V = Volume, m³/mol,

R = Universal gas constant,

$a(T)$, a gas constant, is a function of temperature, described by equation 3,

$$a(T) = \frac{.45724 R^2 T_c^2 \alpha(T)}{P_c} \quad (3)$$

where,

P_c = Critical Pressure, Pa,

T_c = Critical Temperature, K,

V_c = Critical Volume, cm³/mol,

and $\alpha(T)$ is a function of temperature, described by equation 4,

$$\sqrt{\alpha} = 1 + m(1 - \sqrt{T/T_c}) \quad (4)$$

b is a constant for the selected fluid as described by equation 5,

$$b = \frac{.07780 R T_c}{P_c} \quad (5)$$

m is a function of the acentric factor, ω , which is equal to 0.2249 for CO₂ [14].

$$m = .37464 + 1.54226\omega - .26992\omega^2 \quad (6)$$

The equation of state can also be expressed in terms of the compressibility factor, z :

$$z^3 - (1 - B)z^2 + (A - 3B^2 - 2B)z - (AB - B^2 - B^3) = 0 \quad (7)$$

Where,

$$z = PV / RT \quad (8)$$

$$A = aP / (RT)^2 \quad (9)$$

$$B = bP / RT \quad (10)$$

Here constants A & B are dependent on the values of the constants a & b . Cubic Equation 7 is solved to get one real root that gives the molar volume from which the density is obtained.

The Chung et al. method [16] is one of the widely used methods to find the viscosity of dense gases. This method includes density along with temperature and pressure, as the input for calculating the viscosity. Chung et al. suggested the following expression for describing the fact that the fluid has a high density for high pressure,

$$\mu = \frac{\mu_1^* (36.344)^* \sqrt{MT_c}}{V_c^{2/3}} \quad (11)$$

Where,

μ = viscosity, μP ,

M = molecular weight, g/mol,

T_c = Critical Temperature, K,

V_c = Critical Volume, cm³/mol,

and

$$\mu_1 = \frac{(T^*)^{0.5}}{\Omega_v} \{F_c [(G_2)^{-1} + E_6 y]\} + \mu^{**} \quad (12)$$

$T^* = 1.2593T_r$ and Ω_v and F_c are defined by equations 13 and 14 respectively.

$$\Omega_v = A_1 (T^*)^{-B_1} + C_1 \exp(-D_1 T^*) + E \exp(-F_1 T^*) \quad (13)$$

where $A_1=1.16145$, $B_1=0.14874$, $C_1=0.52487$, $D_1=0.77320$, $E=2.16178$ and $F_1=2.43787$

$$F_c = 1 - 0.2756\omega \quad (14)$$

ω is the acentric factor which is equal to 0.2249 for CO₂ [14].

With molar density, ρ in mol/cc,

$$y = \rho V_c / 6 \quad (15)$$

$$G_1 = \frac{1 - 0.5y}{(1 - y)^3} \quad (16)$$

$$G_2 = \frac{E_1 \{ [1 - \exp(-E_4 y)] / y \} + E_2 G_1 \exp(E_5 y) + E_3 G_1}{E_1 E_4 + E_2 + E_3} \quad (17)$$

$$\mu^{**} = E_7 y^2 G_2 \exp[E_8 + E_9 (T^*)^{-1} + E_{10} (T^*)^{-2}] \quad (18)$$

and the parameters E_1 to E_{10} are shown in Table 1.

Table 1. Chung et al. Coefficients to Calculate $E_i = a_i + b_i \omega$ [14]

i	a_i	b_i
1	3.324	50.412
2	1.210E-3	-1.154E-3
3	5.283	254.209
4	6.623	38.096
5	19.745	7.630
6	-1.900	-12.537
7	24.275	3.450
8	0.7972	1.117
9	-0.2382	0.06770
10	0.06863	0.3479

3.2. Heat Transfer Model

Lyons et al. [17] illustrated through plots of temperature in compressible air drilling operations that temperature of the compressed air at any position in the borehole and inside the tubing is approximately the geothermal temperature at that depth. This is because air/gas has poor heat storage capacities relative to drilling mud and turbulent flow conditions in the annulus is very efficient in transferring heat from surface of borehole to the flowing air/gas in the annulus. Therefore, temperature of CO₂ in the annulus and the tubing can be assumed to be the geothermal temperature as a first approximation. For the case studies that will be discussed subsequently, the temperature profile in the annulus and the tubing has been calculated based on this approximation.

An attempt was made for calculating the temperatures of CO₂ in the tubing and the annulus based on the analytical model proposed by Holmes and Swift [18]. This has been discussed in detail in Appendix C.

3.3. Circulation Model

The density and viscosity values obtained from the PVT model are needed as inputs for the circulation model that calculates the hydrostatic pressure and frictional pressure

losses in the tubing and the annulus at each depth and provides the value of the bottomhole pressure. The frictional losses are calculated based on the equations for turbulent Newtonian fluid (Bourgoyne et al [19]).

The model also calculates important drilling parameters such as the cuttings transport ratio (CTR) and the jet impact force. CTR is defined as [19]:

$$CTR = 1 - (V_{slip} / V_{ann}), \quad (19)$$

where,

V_{slip} = slip velocity of cutting, ft/sec

V_{ann} = fluid velocity in the annulus, ft/sec

A positive CTR indicates that the cuttings are transported to the surface. It is an excellent measure of the cuttings carrying capacity of a drilling fluid. In general, it is desirable to have $CTR > 0.7$ in the vertical section, and > 0.9 in the horizontal section, for optimum hole cleaning [20]. For low values of cuttings transport ratio, the concentration of cuttings remaining in the borehole increases. This in turn leads to a high circulation bottomhole pressure and a low penetration rate [19].

Another important drilling performance parameter is the impact force of the fluid jets once they exit the nozzle. The cleaning action can be maximized by maximizing the total hydraulic impact force of the jetted fluid against the bottom of the hole [19]. The jet impact force F_j is given by the following equation [19]:

$$F_j = 0.01823 C_d q \sqrt{\rho \Delta p_b} \quad (20)$$

where,

C_d = discharge coefficient

q = flow rate, gpm

ρ = density of fluid, lb/gal

Δp_b = pressure drop across the nozzle, psi

3.4. Assumptions of the Model

The following simplifying assumptions are needed in order to solve various model equations while preserving the essential physics of the flow process.

1. Temperature of CO₂ in the annulus and the tubing follows the geothermal temperature.
2. The pressure losses are calculated by considering CO₂ as a Newtonian fluid in turbulent flow.
3. The total pressure loss across the mud-motor/turbo-drill, the MWD array and the nozzles is assumed.
4. No inflow of formation water.

3.5. Methodology

The model developed in this study is used to simulate potential scenarios during drilling with supercritical CO₂ as a drilling fluid. The possibility of maintaining the bottomhole pressure (BHP) lower than the reservoir pressure by controlling the choke is simulated. The model simulations start on the annulus side, at the choke, where the user specifies the choke pressure and the surface temperature. The well is segmented into smaller elements, each of length, ΔL . The pressure at each location along the annulus is determined by first calculating pressure losses and then integrating the hydrostatic pressure due to the overlying fluid. The calculations are sequentially performed for each element from the surface down to the bottom of the well. The bottomhole pressure, along with the knowledge of pressure drop across the bit nozzles, allows the calculation of

tubing pressure values at each location upstream of the bit to the surface. Figure 4 illustrates a finite element considered in the numerical model. The flowchart that describes the working of the model is shown in Figure 5.

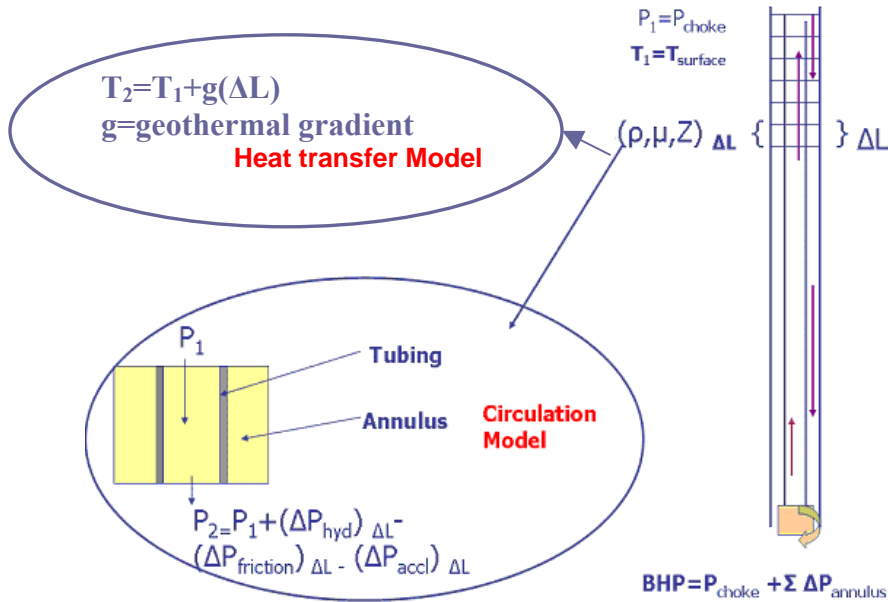


Figure 4. Example of a Finite Element Considered in the Model

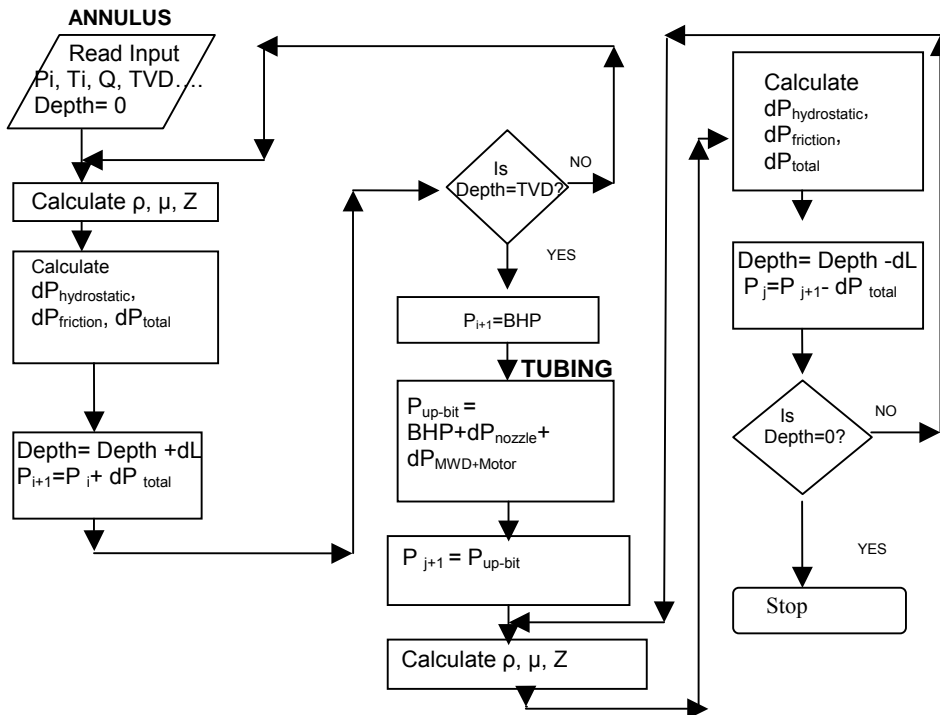


Figure 5. Flowchart of the Proposed Model

CHAPTER 4

CASE STUDY APPLICATION

4.1. Operations Summary

The problems described in Section 1.1. that occurred during the drilling operation in the example depleted gas well may be overcome by using CO₂ and nozzle sizes such that the pressure drop across the bit is large enough to force a phase change. The proposed system is designed such that liquid CO₂ from bulk supply is pumped through the coiled tubing using a high-pressure pump to a pressure level above its critical pressure (1074 psia). As it enters the tubing, CO₂ heats up and becomes supercritical. On its circulation downhole the supercritical phase powers the downhole motor that turns the bit. As the supercritical CO₂ exits the nozzles attached to the drill-bit, the large pressure drop across the nozzle is expected to flash it to a gas phase in the annulus, resulting in a low bottomhole pressure and low annular pressure gradient. CO₂ in the gas phase is expected to carry the cuttings to the surface where the solids are separated at the separator following the choke manifold. Ideally, there is a need to incorporate a CO₂ compression unit following the returns handling system, in order to prevent the venting of CO₂ into atmosphere and to reduce the amount of CO₂ needed for the drilling operations.

4.2. Input Data [1]

- **Well Data**

The vertical section of the well consisted of a 7.625" production casing. The sidetrack started at 11,286' and terminated at 14,304', 0.5 deg from the vertical. A 4.5" casing was placed through the sidetracked length and cemented just above the target zone. The

depth to be drilled was from 14,304 to 14,364' using a 3.875" drill-bit. The wellbore schematic is illustrated in Figure 6.

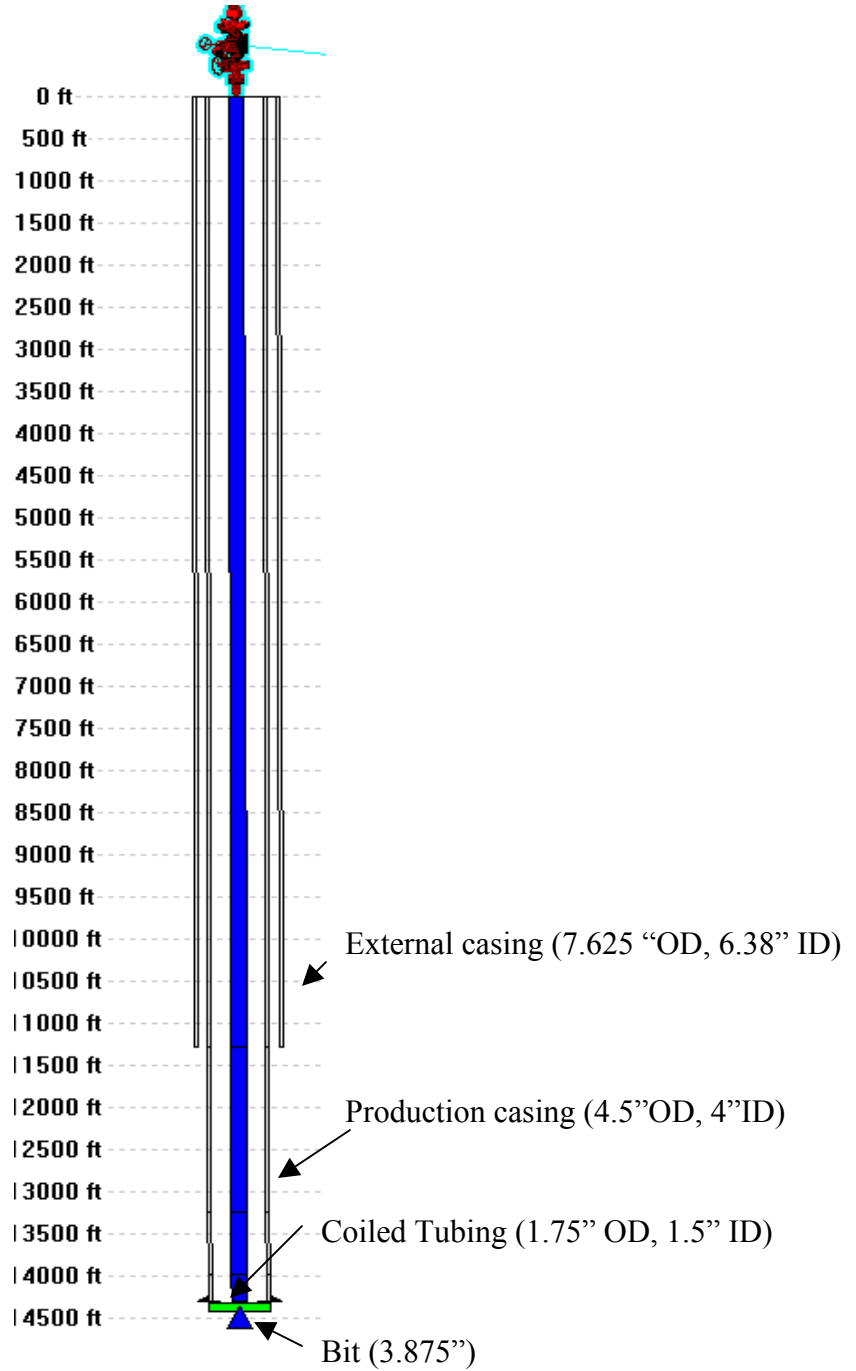


Figure 6. Wellbore Schematic for Example Case Study

- **Coiled Tubing and Bottomhole Assembly**

The coiled tubing used for the project had a 1.75” OD, 0.135” wall thickness and 80,000 psi minimum yield strength. The BHA had a diameter of 2.875” and consisted of a specially designed high pressure downhole motor.

- **Drilling Fluid**

The drilling fluid considered for the simulation study is carbon dioxide which will be stored and injected as a liquid.

The main input parameters to get a bottomhole pressure of 400 psi so as to achieve an underbalance of 300 psi are indicated in Table 2. The choke pressure and /or flow rate of gas is varied to achieve the target bottomhole pressure.

Table 2. Main Input Parameters for the Model for BHP = 400 psi

Choke Pressure, psia	100
Surface Temperature, deg.F	60
Flow rate of gas, scfm	1500
(Equivalent flow rate of liquid CO ₂ ,lbm/min)	(174)
Geothermal gradient, deg.F/ft	0.016

4.3. Simulation Results and Discussions

1. The bottom-hole pressure obtainable for the CO₂ system is 400 psi with an underbalance of 300 psi. In comparison, the foam had created an overbalance of 1938 psi with a BHP of 2638 psi (this case was modeled using WELLFLO 7 and is discussed in Chapter 5). The frictional pressure drop in the annulus is 139 psi.
2. Figure 7 illustrates the calculated variations of CO₂ density with pressure at different temperatures. The plot at 50 °F corresponds to the liquid phase of CO₂. With increase in temperature and pressure, CO₂ attains the supercritical phase

properties. However, with a sharp drop in pressure, such as, at the bit-nozzles, the density drops to that of the gas phase, typically ranging from 1.0 to 0.5 ppg.

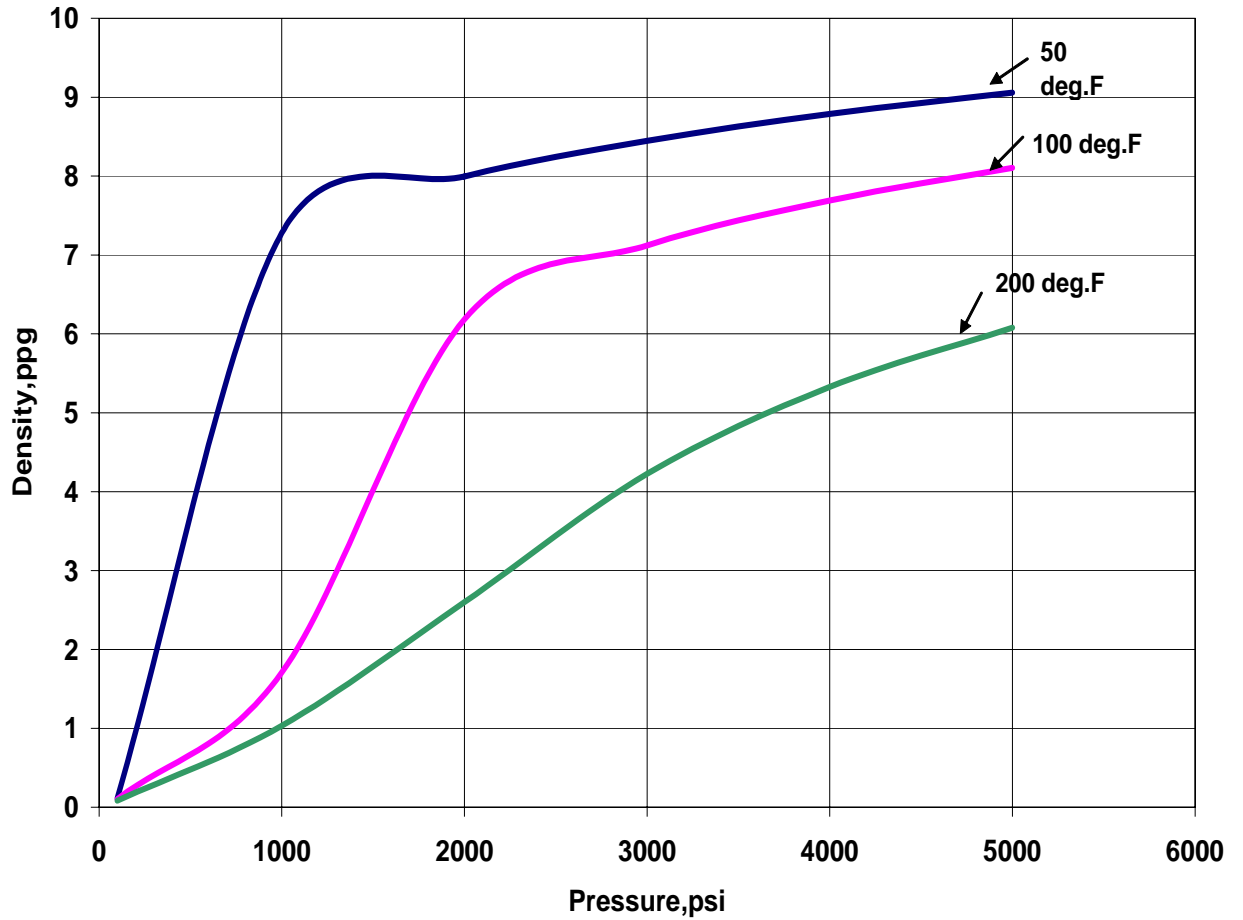


Figure 7. Variation of Density of CO₂ with Pressure at Different Temperature Values

3. Figure 8 illustrates the variation of the viscosity of CO₂ with temperature at different pressure values. The viscosity values for the supercritical phase are comparable to that of a gas, and, as a result turbulent flow conditions are easily achieved.

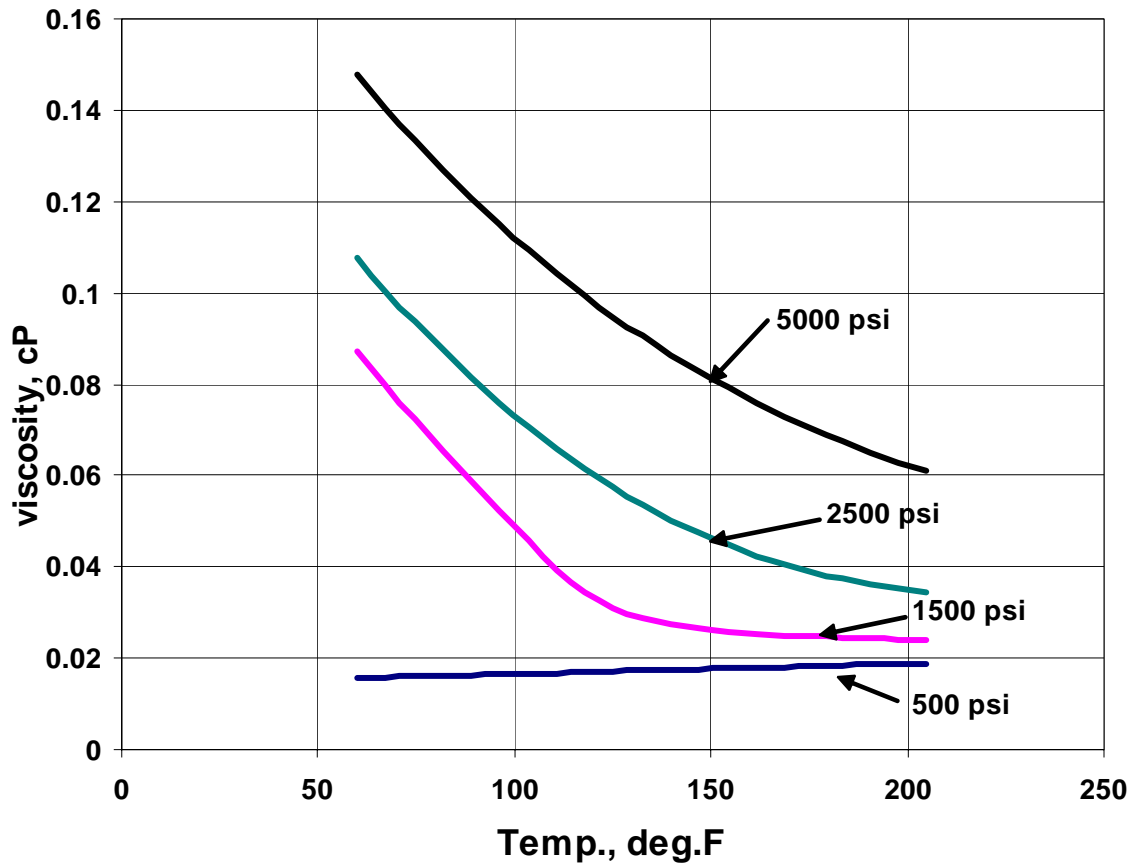


Figure 8. Variation of Viscosity of CO₂ with Temperature at Different Pressure Values

4. Figure 9 illustrates the variation of the density of CO₂ with depth in the tubing and annulus. It is observed that it is possible to obtain a sharp contrast in the density values in the tubing and the annulus when CO₂ is used as the drilling fluid. The higher density in the tubing is necessary for generating sufficient torque in the motor, while the lower density in the annulus allows the underbalanced conditions. This is a very important result as density of CO₂ strongly influences the resulting circulating pressures in the tubing and the annulus and this can be observed in Figure 10.

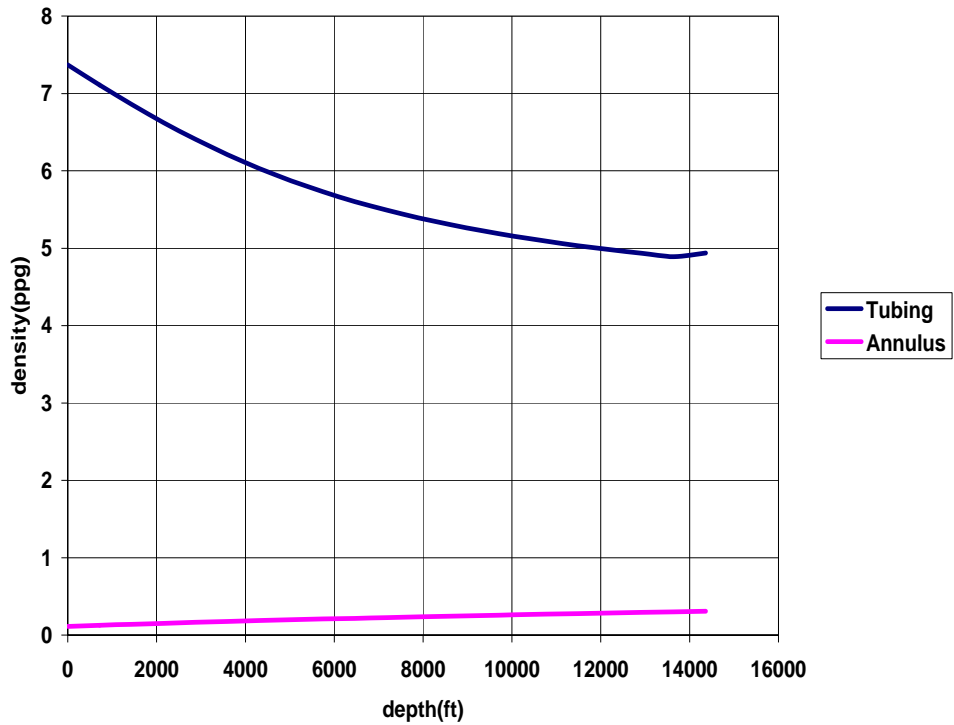


Figure 9. Variation of CO₂ Density with Depth

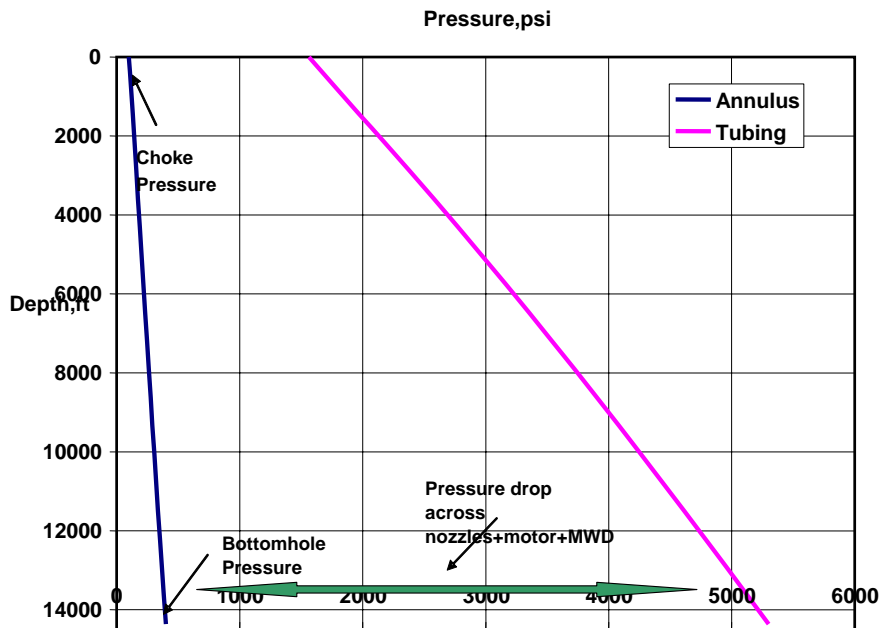


Figure 10. Variation of Circulating Pressure with Depth

5. Figure 10 illustrates the circulating pressures in the tubing and the annulus, respectively. The pressure profile in the annulus is attractive from an underbalanced drilling perspective. The large pressure drop across the nozzles generates the desirable jet impact force.
6. Figure 11 illustrates the variation of bottomhole pressure with choke pressure changes. It is clearly seen that the surface choke plays a crucial role in maintaining underbalanced conditions in the annulus when CO₂ is used as a drilling fluid. One can adjust the choke to readily change the annular pressure profile from underbalanced to balanced to overbalanced conditions.

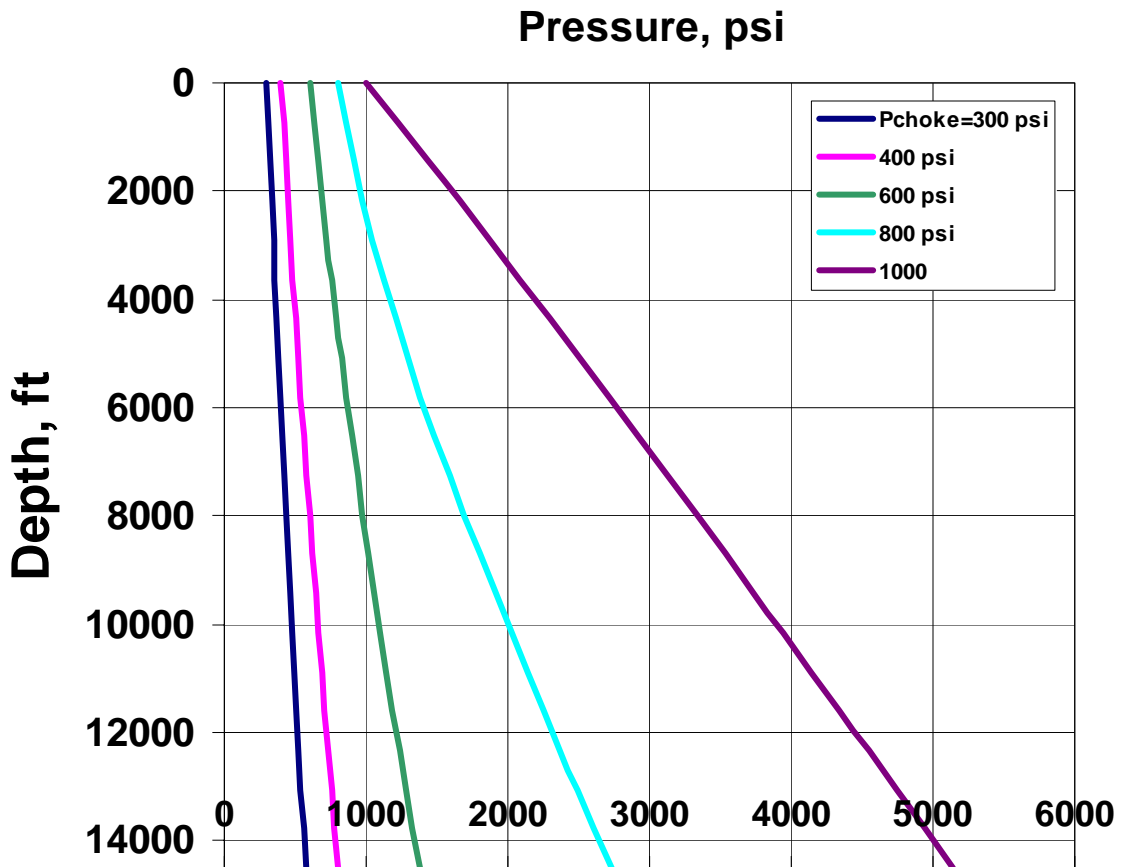


Figure 11. Variation of Bottom-hole Pressure with Choke Pressure

7. Figure 12 illustrates the variation of cuttings transport ratio (CTR) with depth for cutting sizes of 0.1, 0.05 and 0.01 inches, respectively. The annular velocities are higher at shallower depth which shows higher CTRs. The size of the cuttings is generally small in an underbalanced drilling operation. Also, the jetting action of CO₂ is expected to further reduce the size of the cuttings.

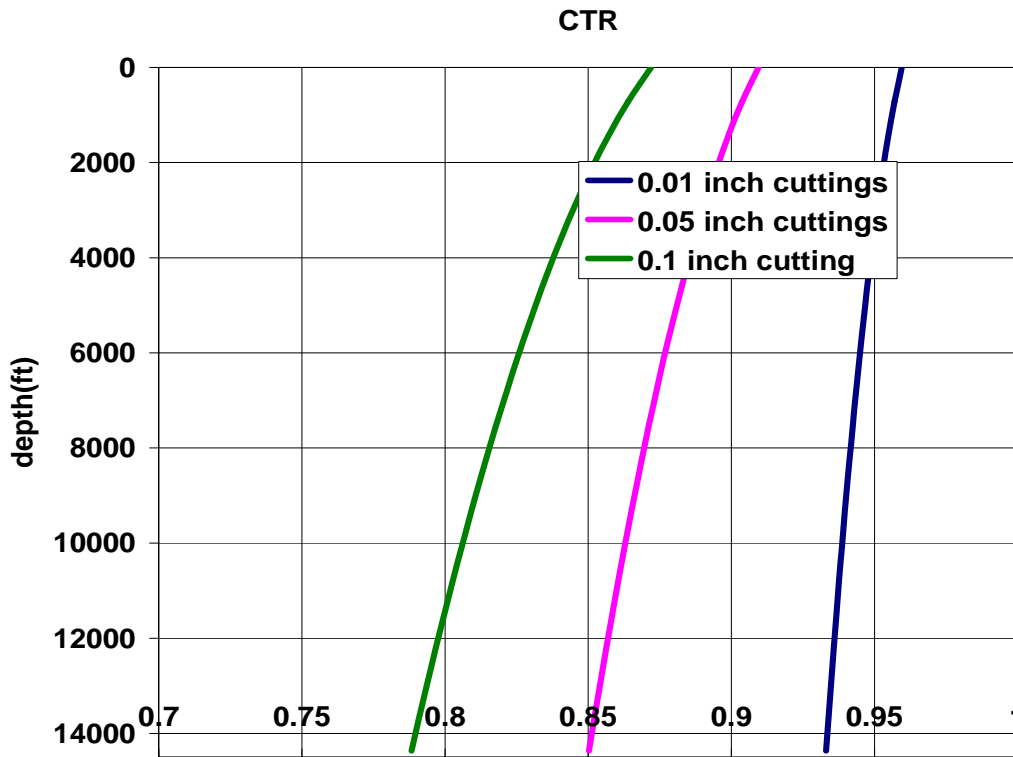


Figure 12. CTR Variations with Depth and Cuttings Size

8. The jet impact force generated by CO₂ expanding through the nozzles (5000 psi) is 1564 lbf. This is calculated based on the density change across the nozzle.

CHAPTER 5

WELLFLO 7 MODELING AND RESULTS

WellFlo7, a NeoTec product, is an industry-standard steady state multiphase flow analysis tool used in UBD well design [23]. It contains a compositional module where the user can specify the equation of state and other correlations to calculate the PVT based properties of the drilling fluid. Because an accurate prediction of the phase behavior of CO₂ is important for our system, WellFlo7 was selected for comparison of the results from the model. Also, the proposed model does not contain iterations and WellFlo7 performs rigorous iterations for target convergence and therefore a comparison of results with WellFlo7 becomes necessary.

5.1. About WellFlo 7 [23]

The user is allowed to design or monitor a UBD well by simulating the fluid flows that occur. Drilling fluids can be any gas, including nitrogen (with or without impurities); water, including brines; hydrocarbon liquids, including diesel and native oils; or aqueous foams. Reservoir fluid production can be specified to occur from a single location, multiple locations or distributed per foot or per meter over any number of defined intervals. Contributing flow rates can be specified as a fixed rate or computed using an IPR. Furthermore, flow can be defined as “in flow”, “out flow” or “free flow”, where flow is entering, leaving, or determined by the pressure differential (i.e. if the bottom-hole pressure is higher than the reservoir static pressure, then you have out flow). All produced reservoir fluids are commingled with the injected drilling fluid(s) on either a compositional or non-compositional basis. Provision exists for taking into account the

pressure drop in the drill string due to the BHA. Pressure losses through the nozzles of the BHA can be specified or calculated and the motor input is reported as an equivalent liquid volumetric rate. Continual velocity checks are performed as the calculations step through the well. In addition, the liquid volume fraction is reported at that point. Input data can be specified using units familiar to drilling engineers (i.e. US gal/min or litres/min for liquids, and scf/min or Sm³/min for gases). Specialized plots such as bottom-hole pressure versus gas injection, liquid transit time, motor equivalent liquid volume versus injection rate, etc, are available in addition to the standard well hydraulics plots.

All calculations are performed using the stepwise calculation procedure for optimum results. Step sizes can be controlled by the user, or the software can be directed to optimize the step size. Pressure calculations can be performed by assuming a temperature profile. Wellhead and bottom-hole temperatures can be entered to define a linear temperature profile or a detailed temperature versus depth profile can be supplied.

5.2. Comparison of Results from Proposed Model and WellFlo 7

Before comparing the results from the proposed model with WellFlo 7 for drilling with CO₂, the case for drilling with foam of nitrogen and water was modeled. 900 scfm nitrogen and 0.75 bpm KCL water with foaming agent was used to generate a 65 quality foam [1]. The choke pressure was set to 100 psi. The resulting pressure profile is shown in Figure 13. The resulting bottomhole pressure is 2638 psi, which creates a condition of severe overbalance in the annulus. The friction in the annulus is 728 psi which is much higher than with CO₂ and the hydrostatic head contribution is 1840 psi. Figure 14

illustrates the excellent cuttings carrying capacity of foam. This is done for cuttings sizes of 0.1 inch and 0.2 inch.

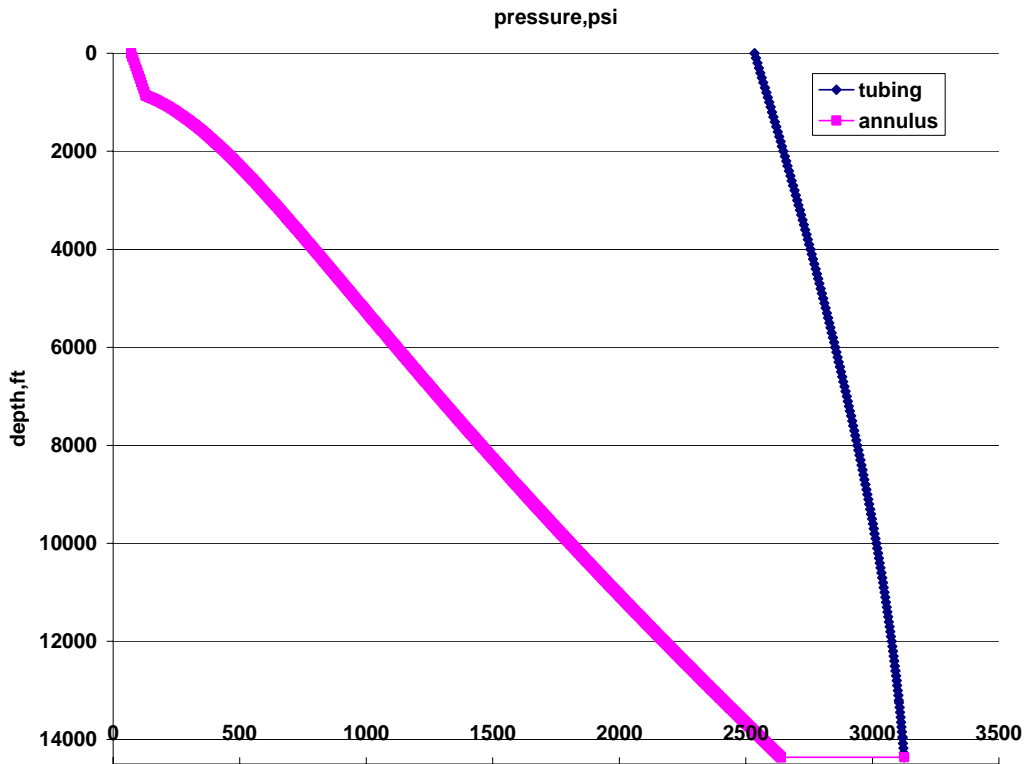


Figure 13. Circulating Pressure Profile of Foam of Nitrogen and Water

Results from figure 14 confirm that foams have excellent hole cleaning capacity. They are therefore used frequently in UBD operations. Foams are an expensive option in comparison to the common drilling fluids used in underbalanced drilling. However, for a very low pressured reservoir, they are unable to maintain underbalance in the wellbore as indicated by the pressure profile in Figure 13. Foams are formed by the addition of surfactant to a mixture of nitrogen and water. The foam breaks close to the surface resulting in a drop in CTR. This is because its quality increases towards the surface due to the decrease in pressure and the gas fraction in the foam increases.

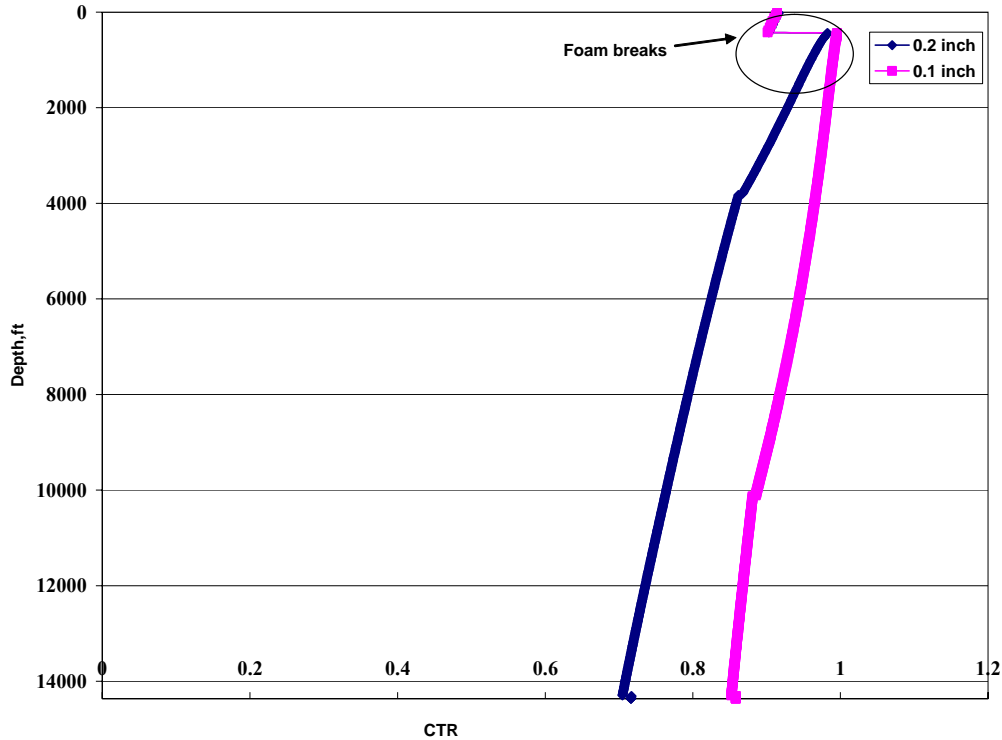


Figure 14. Cuttings Transport Ratios for 0.1” and 0.2” Cuttings for Foam

Results obtained for the case study example using the proposed model were compared with the results from WellFlo 7 to determine the accuracy of the model developed. CO₂ was modeled as a compositional fluid because it suitably described its phase changes on the tubing side. The drilling profile and other parameters were entered by assuming a linear temperature profile both on the annulus and the tubing side. The input parameters are same as indicated in Table 2. Figure 15 illustrates the circulating pressure profile for the case study using WellFlo 7. On comparing with Figure 10, the model underestimates the injection pressure needed to get the necessary pressure drop across the BHA and the bottomhole pressure by 37 psi. The WellFlo results indicate that with CO₂, the pressure profile needed to get underbalanced conditions can be achieved. Also, denser phase in the tubing can be achieved. The friction pressure drop in the annulus is 107 psi compared to

139 psi predicted by the proposed model. This comparison is done by assuming the same choke pressure and flow rate.

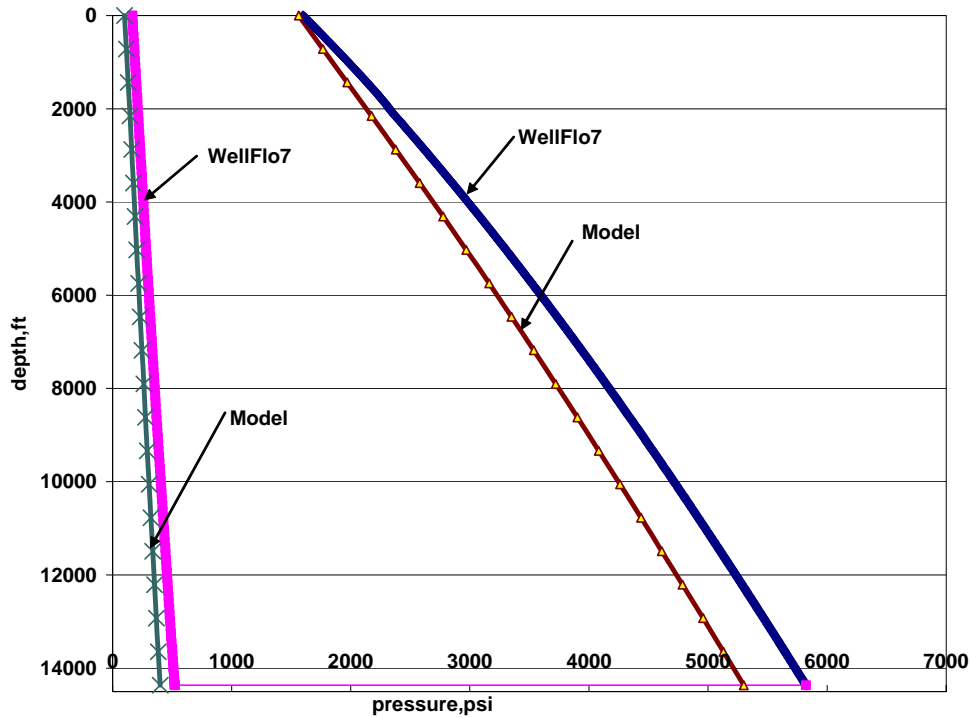


Figure 15. Comparison of circulating pressure profile from Model and WellFlo 7

Figure 16 illustrates the comparison of the frictional pressure drop values with choke pressure for the same flow rate of gas, from the model and WellFlo7. As the choke pressure is increased, the bottomhole pressure also increases which causes a reduction in the annular velocity of the drilling fluid. This causes a reduction in the frictional pressure drop in the annulus.

Figure 17 illustrates the comparison of the frictional pressure drop values with gas flow rate for the same choke pressure, from the model and WellFlo7. A higher gas flow rate results in higher circulating annular velocity which causes higher frictional pressure drop.

As the gas flow rate is increased, the difference in the pressure drop values predicted by the model and WellFlo7 also increases.

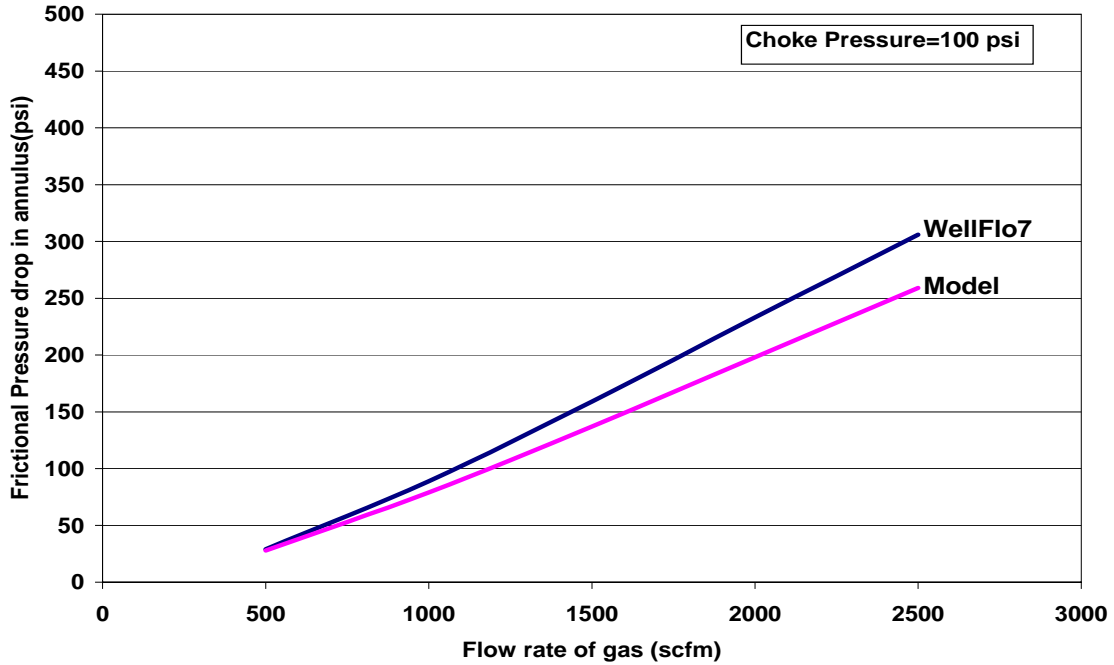


Figure 16. Comparison of Frictional Pressure Drop with Choke Pressure from Model and WellFlo 7

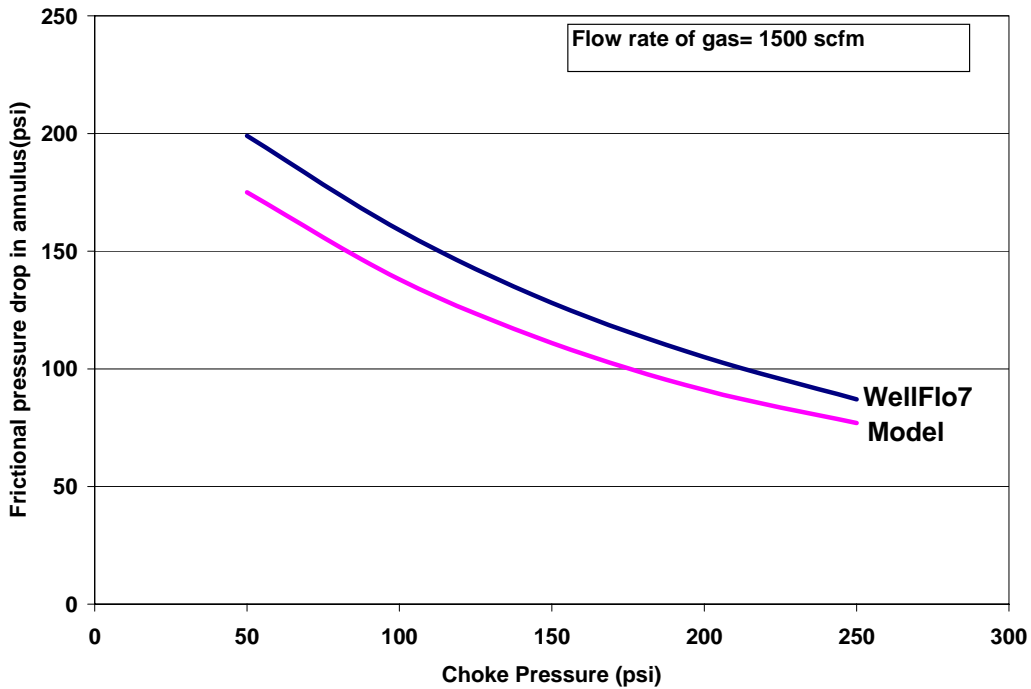


Figure 17. Comparison of Frictional Pressure Drop with Gas Flow Rate from Model and WellFlo 7

A comparison of density values obtained from the model and WellFlo7 for a combination of pressure and temperature values is shown in Figure 18. The density values predicted by the model closely match the values calculated by WellFlo7. This increases the confidence in the density predictions by the PVT model. Density is an extremely important property as it largely determines the circulating pressure profile. This is definitely an encouraging result.

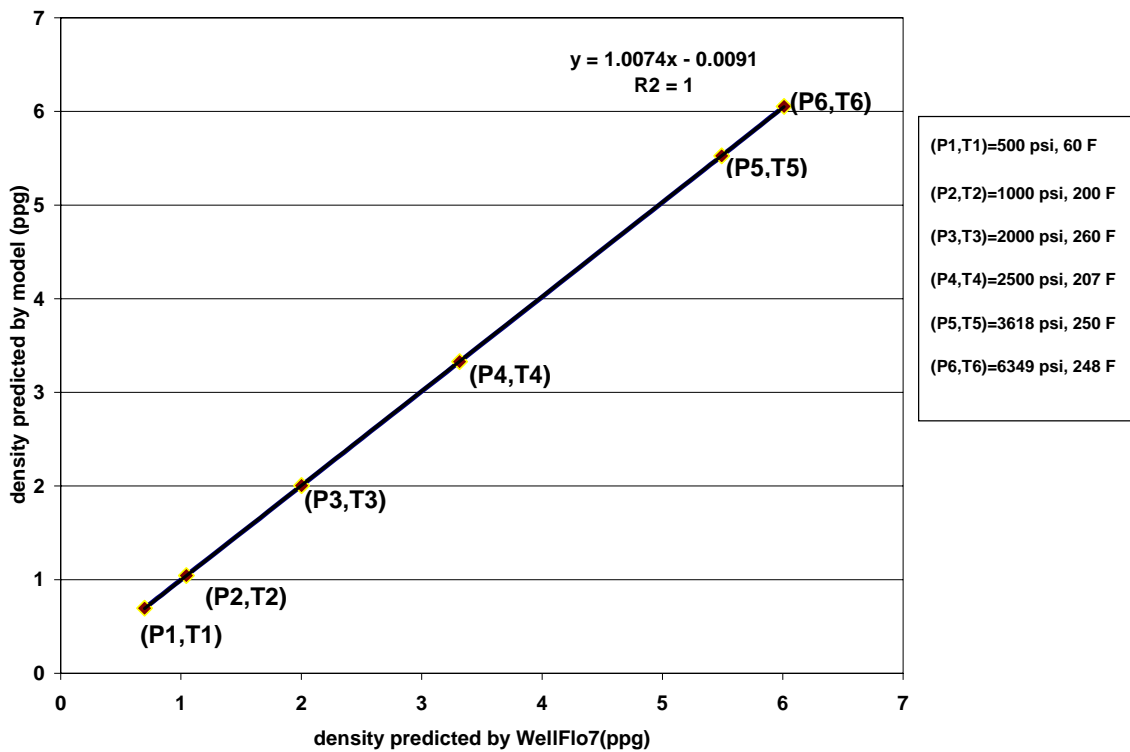


Figure 18. Comparison of Density Predictions from Model and WellFlo 7

Figure 19 illustrates the change in density of CO₂ in the tubing and the annulus. It agrees with our expectation of being able to achieve a higher density in the tubing and a lighter fluid in the annulus. WellFlo 7 does not identify the supercritical phase of CO₂ as supercritical, but as a liquid or gas depending on the pressure and temperature. The drop in density in the above plot is due to the transition of liquid phase of CO₂ to the

supercritical phase. However WellFlo 7 identifies supercritical CO₂ beyond this transition phase as liquid until some distance where it sees it as a gas. However, the incapability of WellFlo7 to distinguish the phase changes does not affect the results as the density values predicted by WellFlo 7 closely match that of model as shown in Figure 18.

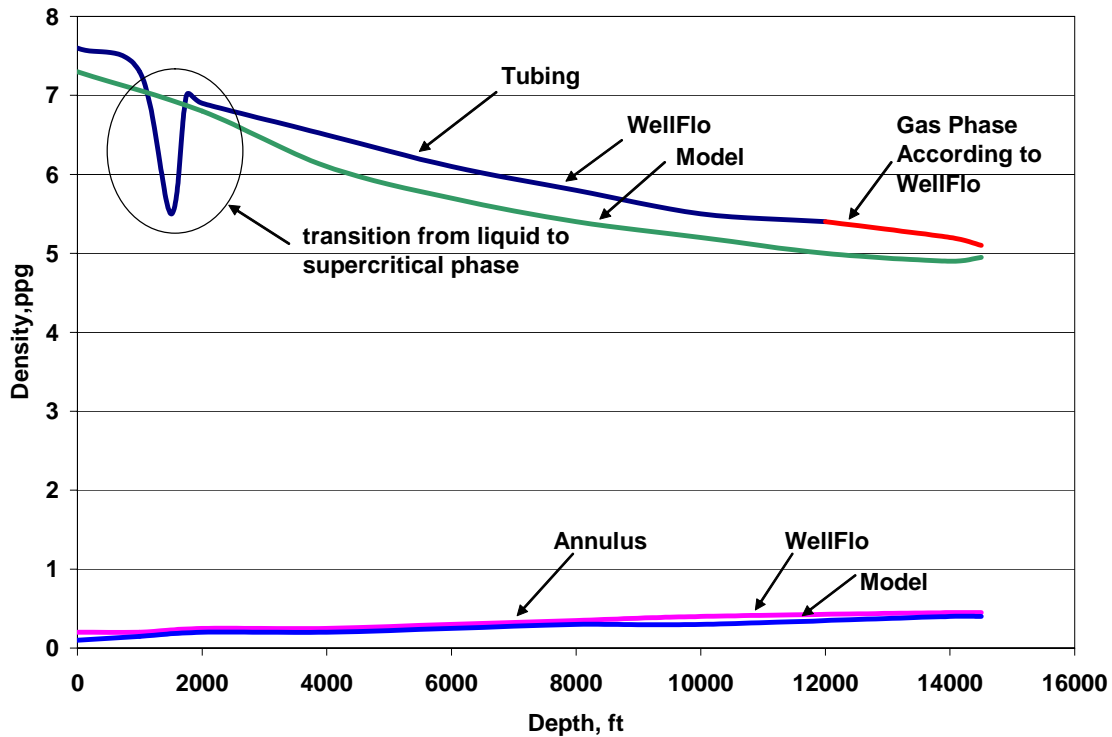


Figure 19. CO₂ Density Variations in the Tubing and the Annulus

A comparison of the CTRs obtained from the model and WellFlo7 as a function of depth is shown in Figure 20. The results predicted by WellFlo7 reaffirm that CTRs would be acceptable for the selected range of cuttings sizes for this CO₂ drilling system. The CTRs predicted by WellFlo7 and the model are fairly close for smaller size cuttings i.e. 0.01 inch and 0.05 inch cuttings. However, for size cuttings greater than 0.1 inch, the difference in the predicted values increases.

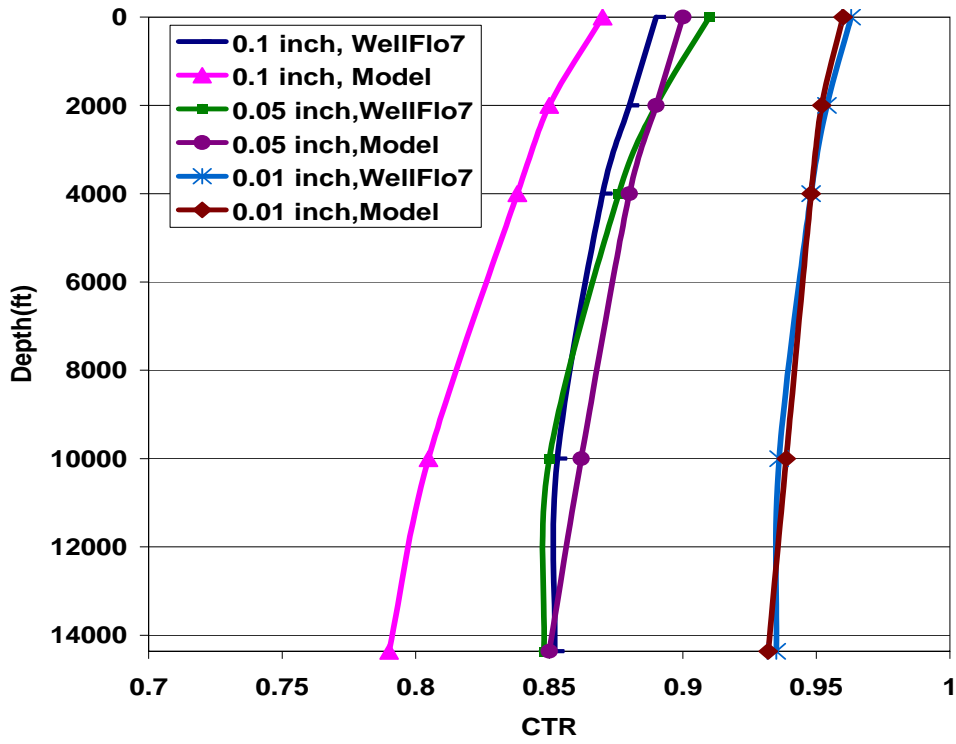


Figure 20. CTR Variations with Depth for Different Sized Cuttings Using WellFlo7

CHAPTER 6

CORROSION PROBLEMS WITH CO₂ AND ITS CUTTINGS CARRYING CAPACITY

6.1. Corrosion Potential of CO₂

Pure and dry CO₂ is non-corrosive. However, if it encounters formation water, carbonic acid is formed which corrodes the metal surface. Iron carbonate is one of the products of the corrosion reaction and is known to have protective properties. The primary environmental factors that affect corrosion rates are: the partial pressure of CO₂, operating pressure and temperature, flow rate of CO₂, water content and contaminants such as hydrogen sulfide and oxygen. Pure CO₂ exerts a very large partial pressure that leads to reduction in pH and increase in the carbonic acid reduction reaction. At temperatures lower than 158 °F, the corrosion rate progressively increases up to an intermediate temperature range (158 to 194 °F) and then the corrosion rate drops [24]. Higher temperatures cause a reduction in the solubility of the protective film of iron carbonate, and this increases pH. However, larger pressure increases solubility and lowers the pH. Higher flow rates increase the transport rates of reacting species to the metal surface and do not allow the protective films to form. Presence of hydrogen sulfide and oxygen can worsen the situation [24]. The physical parameters that affect corrosion rate include water wetting, presence of wax and crude oil, and, characteristics of the corrosion film. If a water-in-oil emulsion forms in an oil/water system, then water is shielded by a continuous oil-film, thus reducing the rate of corrosion. Wettability effect and corrosion inhibition by surface active components of the crude oil can provide protection [25].

In terms of corrosion mitigation, iron carbonate or siderite film is most important. In terms of metallurgy, small quantities of chromium (0.5 wt % to 3 wt %) is beneficial as it promotes the formation of stable, protective chromium oxide film. It is found that V-microalloyed steel containing Cr, Si, Mo and Cu is the most promising composition in terms of corrosion resistance and mechanical properties [24]. Liquid CO₂ is completely dehydrated before injection so internal corrosion of the tubing may not be a problem.

The de Waard and Milliams equation [26] predicts the maximum rate of corrosion or the worst case scenario. The de Waard and Milliams nomogram is a simple form of relationship between ‘potential corrosivity’ and temperature and partial pressure of CO₂ and is illustrated in Figure 21. It also includes a scale for the deposit factor (scale factor) that accounts for the formation of the protective carbonate film that causes reduction in corrosion rate at higher temperature.

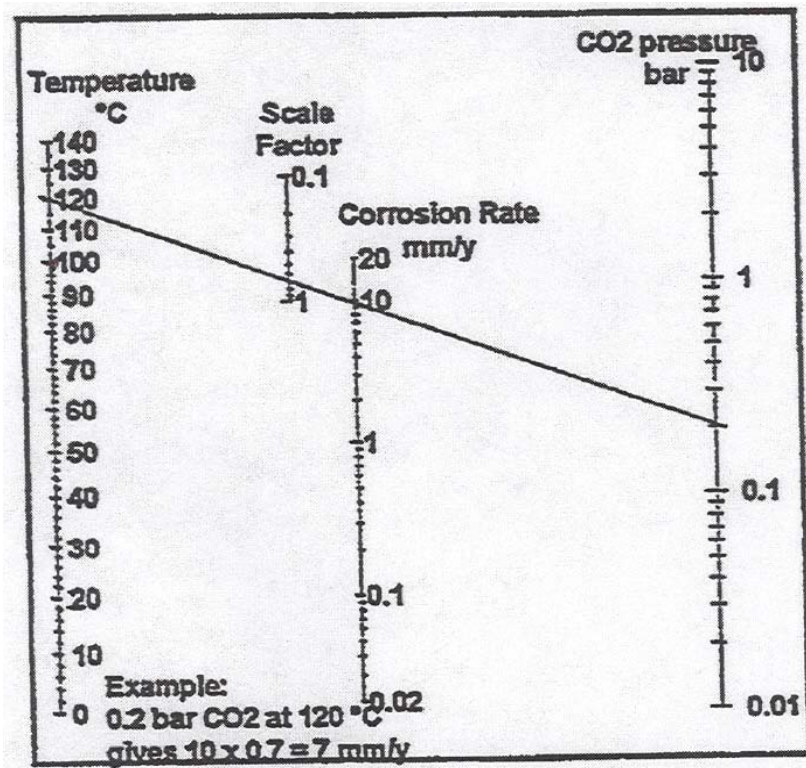


Figure 21. de Waard and Milliams Nomogram [16]

The corrosion rates are expressed in millimeters/year or mils/year. The rate is expressed as a function of pressure and temperature:

$$\log(V_{corr}) = 5.8 - (1710/T) + 0.67 \log(pp_{CO_2}) \quad (21)$$

where,

V_{corr} = corrosion rate in mm/year

T = temperature, K

pp_{CO_2} = partial pressure of CO₂, bar

Above equation does not consider the presence of scale, flow rate, pH and non-ideality of gas. Aaker [22] corrected the de Waard and Milliams equation for scaling and non-ideality of gases. A scale factor (F_{scale}) is taken into account for the formation of protective carbonate films that lead to a reduced corrosion rate at higher temperatures. At temperatures above 140 deg. F one needs to take this factor into account though at temperatures below 140 deg. F its value is taken as 1. Scale factor is given by:

$$\log F_{scale} = (2500/(T - 7.5)) \quad (22)$$

where

T = temperature, K

Fugacity coefficient (a) that takes into consideration the non-ideality of gases at higher pressure is calculated by the following equation. The fugacity of CO₂ (f_{CO_2}) was used in place of partial pressure in the calculations.

$$f_{CO_2} = (a)(pp_{CO_2}) \quad (23)$$

$$\log(a) = P_{total} \left[0.0031 - \left(\frac{1.4}{T} \right) \right] \quad (24)$$

where

P_{total} = Total pressure of the system

T = temperature, K

pp_{CO_2} = partial pressure of CO₂, bar

Based on the work of Aaker [22], the corrosion rates for a CO₂ based drilling system, along the length of the annulus, are illustrated in Figure 22. The variation of choke pressure causes changes in BHP which, in turn, affects the downhole corrosion rates. Higher choke pressure implies higher pressures in the annulus and hence higher corrosion rates.

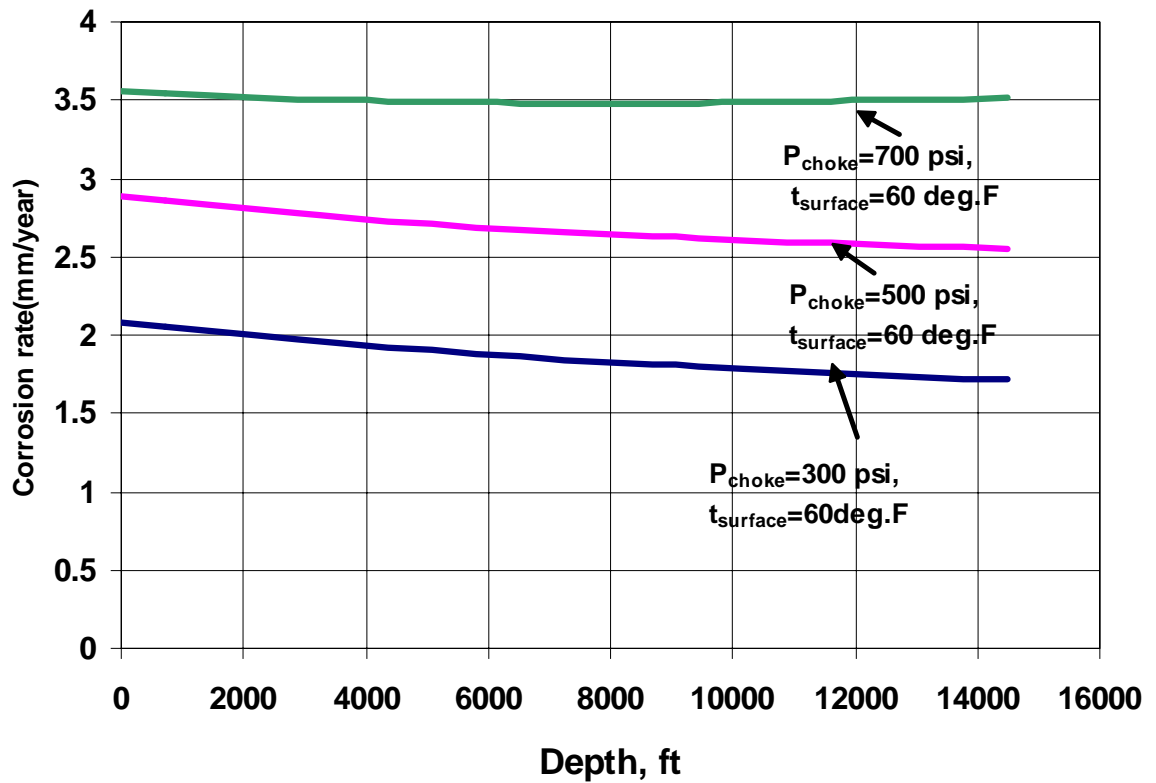


Figure 22. Corrosion Rates Along the Annulus Length for Different Choke Pressures

Corrosion affects the economics of the process and hence it is essential to include the necessary corrosion related steps in the planning phase before the initiation of the project. Detection and monitoring of corrosion rates is essential. Data collection on wells improves the chances of accurately predicting and managing the risks of corrosion. Test coupons, caliper surveys, sonic-thickness logs and probes are some of the options that do not require pulling the tubing out of the hole for inspection.

Since the corrosion rates can be severe under certain downhole conditions, one must look at the available preventive methods. An effective corrosion control program must be designed that may combine 2 or more preventive methods. Corrosion resistant alloys (13% Cr steel, duplex stainless steels) either in the solid form or as a cladding on carbon steel are the most attractive though expensive solution to CO₂ corrosion problem. The most common method of corrosion prevention in the industry is the use of corrosion inhibitor that is designed to cover the metal surface with an oil-wet film. Its concentration can be changed in situ without disrupting any operations. Protective coatings provide a barrier between the metal and the environment. However in presence of solids and high flow rates coatings can be quickly eroded and hence do not offer a reliable solution to the corrosion problem.

6.2. Low Viscosity of CO₂: Potential for Using Thickening Agents

The low viscosity of CO₂ is a concern from the cuttings carrying perspective. Turbulent velocity conditions in the annulus are an alternative for avoiding cleaning problems in the hole, in the absence of high-viscosity of the drilling fluid. However, the increase in the frictional losses in the tubing limits the increment in velocity of the drilling fluid to maintain turbulence in the annulus. The low viscosity of CO₂ is also a concern in fracture

stimulation and EOR projects using CO₂. Hence numerous studies [27, 28, 29, 30 and 31] have been conducted to develop ‘thickeners’ for CO₂.

Enick et al. [27] designed and synthesized thickeners that exhibit high CO₂ solubility and the ability to induce significant increases (2-100 fold) in viscosity. Each candidate thickener contained a CO₂-philic group for enhancing solubility and a CO₂-phobic group to induce intermolecular interactions that resulted in formation of macromolecular structures in solution which were capable of causing tremendous increases in solution viscosity. The thickened solution would be transparent, single-phase and shear-thinning. Xu et al. [28] discuss the utility of fluoroacrylate-styrene copolymer for thickening of CO₂. Fluoropolymers are characterized by environmental persistence, high cost and unavailability in large quantities. Therefore nonfluorous, inexpensive thickeners are currently being designed. Several promising non-fluorous CO₂ soluble polymers have been identified in the literature, including polypropylene oxide and polyvinyl acetate. Bae and Irani [29] conducted a laboratory investigation of the viscosified CO₂ using a commercial silicon polymer and toluene as a cosolvent. The viscosified CO₂ was used in corefloods in Berea and carbonate reservoir cores. The oil recovery obtained was compared to the results of other processes such as neat CO₂ and WAG. It was found that oil recovery is enhanced and CO₂ breakthrough retarded significantly. Enick [21] has conducted a literature review of the studies in this field where it is concluded that a satisfactory thickener has not been identified for field application but the effort is being carried out in this regard. Significant research in this field is ongoing.

Techniques are being developed to “gel” carbon dioxide [31]. Shi et al. [31] have combined concepts of CO₂-philic design and molecular assembly in solution to generate

compounds that gel CO_2 at concentrations below 5 weight %. These compounds have a strong thermodynamic affinity for CO_2 dissolving in it to form gels. Upon removal of the CO_2 , these gels produce free-standing foams with an average diameter smaller than 1 micrometer and a bulk density reduction of 97 % relative to the parent material. Figure 23 illustrates the scanning electron microscope (SEM) images of the foam produced from different gelling compounds in single-phase solutions of CO_2 . The interesting finding is that once the gelling of supercritical CO_2 under high pressure is done to form a semi-solid material, the release of pressure does not change the shape of the material.

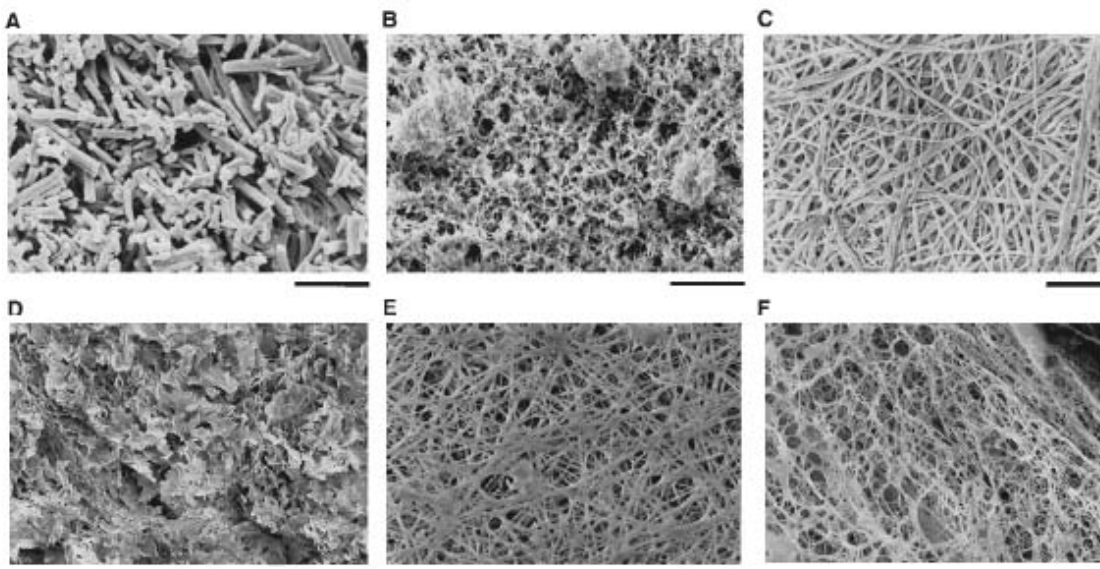


Figure 23. SEM Images of Foam Produced from CO_2 -gels

CHAPTER 7

QUALITATIVE ANALYSIS OF DRILLING WITH SUPERCRITICAL CO₂

7.1. Potential Advantages

Based on the results of the simulation study for the example case study and results from WELLFLO 7, some advantages of using CO₂ as a drilling fluid become apparent.

1. High density of liquid-supercritical CO₂ in the tubing allows the downhole motor to generate necessary torque for satisfactory drilling in the example case study. Also, the jetting action is expected to complement the bit performance and enhance the drilling rates. In addition to lubricating and cooling the bit, it provides pre-cleaning of the tool path and propagation of the cracks induced by the bit [13].
2. Gaseous phase CO₂ in the annulus leads to lower pressure values in the annulus which is very important for an underbalanced drilling operation. The results also indicate that efficient hole-cleaning is achieved in the system as long as cutting sizes are less than 0.05”.
3. The critical temperature (88 deg. F) and critical pressure of CO₂ (1074 psi) are favorable from the point of view of energy requirements.
4. CO₂ is a non-damaging fluid for the formation and does not adversely affect the formation permeability. In fact, it is often used as a fracturing fluid because it improves the fluid conductivity near the wellbore.

7.2. Possible Problems

Despite potential advantages offered by the use of CO₂ as a drilling fluid, some problems are anticipated as described in the following.

- a. If formation water mixes with CO₂ in the annulus, then corrosion rates can be significant. This is a major concern.
- b. Cuttings carrying capacity could be questionable due to the low viscosity of CO₂. However, the results show that as long as turbulent flow conditions are maintained in the annulus and for smaller cuttings, CTRs are favorable. For other situations, there may be a need to increase the viscosity using CO₂ thickeners/viscosifiers.
- c. The NIST data tables [21] indicate that the Joule Thompson coefficient for the CO₂ system is 0.0012 °F/psi, which corresponds to a temperature drop of 8 °F across the nozzles. The Joule Thompson effect, though not significant for the case study, needs to be considered for any possibility of a large temperature drop across the nozzles and the choke.
- d. The CO₂ drilling system requires a specially designed high pressure motor with sealing elements compatible with supercritical CO₂, as it is known to cause swelling of the elastomers. Drilling turbines may offer an attractive alternative to mud-motors.
- e. The system requires high-pressure equipment, including a high pressure pump to inject liquid CO₂, high pressure coiled tubing and specially designed jetting bits that work on the principle of critical flow. This is important because critical flow will definitely occur as a large pressure drop is desired across the nozzles. The working pressure rating of coiled tubing is constrained by its fatigue limits.
- f. CO₂ is a green-house gas and therefore there are environmental issues associated with its discharge to the atmosphere. An alternative is to re-compress the

circulated CO₂, which can be stored for further use as a drilling fluid or for enhanced recovery projects.

7.3. Economic Considerations

The costs for CO₂ vary between \$10/ton to \$50/ton depending on the location of the source such as CO₂ producing reservoirs or power stations. It makes most economical sense to have the source close to the drilling site. Wooten [32] provided a brief outline of methods of supply versus volume requirement:

1. Low Volume or job specific or temporary/ short term injection requirement - Transport Trucks
2. Intermediate volume requirement or remote locations - Investigate installation of small gas extraction system
3. Medium to High Volume or long term project- Source of gas from other gas fields.

UBD wells are drilled after serious front-end engineering as they are expensive wells to be drilled due to the requirement of special equipment and personnel. The incremental surface equipment costs include a high pressure pump, compressors, and separation units, in addition to CO₂ recovery systems. The coiled tubing system, well control system and bottomhole assembly add to the equipment costs. The process may be cost-effective as long as CO₂ can be recaptured after drilling and stored for use as a fracturing fluid or an enhanced recovery treatment. In addition, the benefits associated with underbalanced drilling include the cost savings of the non-productive time associated with conventional drilling, dealing with lost circulation and differential sticking problems [20]. Additional

savings may result from improved drilling rates and elimination of the costs associated with stimulation and cleanup [20].

CHAPTER 8

CONCLUSIONS AND RECOMMENDATIONS

8.1. Conclusions

The work presented is an analysis of the technical feasibility of underbalanced drilling with CO₂ in deep wells using a coiled tubing operation. The system is modeled as a spreadsheet application and applied to a field case study. The results are compared with WELLFLO 7, a flow modeling tool for UBD.

1. The results indicate that drilling with the CO₂ system can provide solutions to the important problems encountered in the example case study. This is very encouraging as it justifies the further development of the proposed technology.
2. Liquid-like density and gas-like viscosity of CO₂ is advantageous in its role as a drilling fluid. These properties allow it to run the downhole motor as well as develop the desired underbalance across the formation face.
3. The large pressure drop across the nozzles allows CO₂ to change to a vapor phase in the annulus which results in accelerated flow velocity for effective borehole cleaning and at the same time maintain underbalanced conditions in the annulus.
4. The surface choke plays a key role in maintaining the desired bottomhole pressure. It allows relatively quick adjustment of bottomhole pressure from underbalanced to overbalanced conditions if the need arises.
5. A corrosion control program is a must for the system and needs careful consideration. It must be a part of the planning process.
6. The drilling cost reduction and reservoir value creation associated with UBD most likely offsets the costs associated with equipment and purchase of bulk liquid CO₂

7. The drilling cost reduction and reservoir value creation associated with UBD most likely offsets the costs associated with equipment and purchase of bulk liquid CO₂.
8. Techniques to recover CO₂ after circulation may make this a value-added process. The recovered CO₂ may then be used for other applications that include EOR and fracture stimulation.

This work has helped to propose a technology that holds potential for the future. The comparison with WELLFLO 7 shows that the model needs to be refined to improve its accuracy. The case study using WELLFLO 7 indicates that CO₂ is an attractive choice for underbalanced drilling operations. Therefore one can conclude that the technical feasibility seems to be proved to an extent. However, this is still an ongoing research and more work is needed in the improvement of the model and its application to a field project.

8.2. Recommendations

Following recommendations are made:

1. A more rigorous iterative technique for the circulation model is recommended to improve its accuracy.
2. A finite-difference approach is recommended for the modeling of the temperature profile in the tubing and the annulus.
3. Techniques for recovery of the circulated CO₂ need to be researched to make it a more economical viable process.
4. A thorough economic analysis of the proposed technology is recommended.

REFERENCES

1. Hilton, D., Pruet Production Co., Personal Communication
2. Phase Diagram of carbon dioxide
Source: <http://www.chemicallogic.com/co2tab/downloads.htm>
3. Phase change of carbon dioxide to supercritical state,
Source: www.firstscience.com
4. Hydrate formation diagram of gases,
Source: www.telusplanet.net/public/jcarroll/HYDR.HTM
5. Bennaceur K., Monea M., Sakurai S., Gupta N., Ramakrishnan T.S., Randem T. and Whittaker S., "CO₂ Capture and Storage", Oilfield Review, 2004
6. Friedman B.M., Wissbaum R.J. and Anderson S.P., " Various recovery processes supply CO₂ for EOR projects", Oil and Gas Journal, Aug 23, 2004
7. "CO₂ EOR Technology", Dec 2004
www.fe.doe.gov/programs/oilgas/publications/eor_co2/CO2brochure2004.pdf
8. Beyer A.H., Millhone R.S. and Foote R.W., "Flow Behavior of Foam as a Well Circulating Fluid", SPE 3986, Oct 1972
9. Bennion D.B., Thomas F.B., Bietz R.F. and Bennion D.W., "Underbalanced Drilling: Praises and Perils", SPE 52889, April 1996
10. Suryanarayana, P.V., Rahman, S, Natarajan, R., and, Reiley, R.: "Development of a probabilistic model to estimate productivity improvement due to underbalanced drilling", paper IADC/SPE 81639 presented at Underbalanced Tech and Exhibition, March 2003
11. Scherchel S.R. and Graves D.G., "Underbalanced-Directional Drilling with Coiled Tubing- Challenges and solutions", paper SPE 37062, Nov 1996
12. Thatcher D.A.A, Szutiak G.A. and Lemay M.M., "Integration of Coiled-Tubing Underbalanced- Drilling Service to Improve Efficiency and Value", SPE 60708, April 2000
13. Kolle, J.J: "Coiled-Tubing Drilling with Supercritical Dioxide", paper SPE 65534 presented at SPE/CIM International Conference on Horizontal Well Technology, Canada, Nov 2000
14. Smith J.M., Van Ness H.C. and Abbott M., "Introduction to Chemical Engineering Thermodynamics", 2004

15. Carroll J.J. and Boyle T.B., "Calculation of Acid Gas Density in the Vapor, Liquid and Dense Phase Region", Presented at the 51st Canadian Chemical Engineering Conference, Oct 2001
16. Poling, B.E, Prausnitz, J.M, and, O'Connell, J.P: "Properties of gases and liquids", 5th Ed, McGraw Hill, 2002
17. Lyons W.C., Guo B. and Seidel F.A., "Air and Gas Drilling Manual", 2nd edition, McGraw-Hill, 2001
18. Holmes, C.S. and Swift, S.C; "Calculation of Circulating Mud Temperatures", paper SPE 2318, JPT, 670-674, June 1970
19. Bourgoyne A.T., Chenevert M.E., Millheim K.K. and Young Jr., : "Applied Drilling Engineering", SPE Textbook Series, (Eds) Evers J.F and Pye D.S, Ninth Printing, 2003
20. Suryanarayana, P.V., Smith, B., Hasan, ABM, Leslie, C., and, Pruitt, R: "Basis of Design for Coiled tubing Underbalanced Through-Tubing Drilling in Sajaa Field", paper IADC/SPE 87146 presented at IADC/SPE Drilling Conference, Dallas, March 2004
21. Lemmon, E.W., McLinden, M.O., and Friend, D.G.: "Thermophysical Properties of Fluid Systems" in *NIST Chemistry WebBook, NIST Standard Reference Database Number 69*, Eds. W.G. Mallard and P.J. Lindstrom, November 1998, National Institute of Standards and Technology, Gaithersburg MD, 20899
22. Aaker, G.A, "Corrosion Prediction", Engineering Services, L.P.
URL: <http://www.engineering-experts.com/co2.html>
23. WellFlo 7, Neotechnology Consultants, Technical and User Documentation
24. Kermani M.B and Morshed A; "Carbon Dioxide Corrosion in Oil and Gas Production-A Compendium", Corrosion, Vol 59, No.8, 2003
25. Lotz. U et al., "The effect of type of Oil or Gas Condensate on Carbonic Acid Corrosion", Corrosion, Vol. 47, No.8, 1991
26. CO₂ Corrosion in Oil and Gas Production-Selected Papers, Abstracts, and References", Eds. Newton, L.E, Jr. and Hausler, R.H., an official NACE Publication, 1984
27. Enick R.M., Beckman E.J., Shi C., Huang Z., Xu J., Kilic S., "Direct Thickeners for Carbon Dioxide", SPE 59325, April 2000

28. Xu J., Enick R.M., Wlaschin A., “Thickening Carbon Dioxide with Fluroacrylate-Styrene Polymer”, SPE 84949, June 2003
29. Bae J.H. and Irani C.A., “A Laboratory Investigation of Viscosified CO₂ Process”, paper SPE 20467, April 1993
30. Enick R.M., “A Literature Review of Attempts to Increase Viscosity of Dense Carbon Dioxide”, under DOE contract DE-AP26-97FT25356, Oct 1998
31. Shi C., Huang Z., Kilic S., Xu J., Enick R.M., Beckman E.J., Carr A.J., Melendez R.E. and Hamilton A.D., “The Gelation of CO₂ : A Sustainable Route to the Creation of Microcellular Materials”, Science magazine, Vol 286, Nov 1999
32. James Wooten, Blade Energy Partners, *Personal Correspondence*.

APPENDIX A

PROPERTIES OF CARBON DIOXIDE

a) Critical Properties:

Critical Temperature: 88 deg. F

Critical Pressure: 1074 psia

Critical Density: 29.2 lb/cu ft

Critical Volume: 94.07 cc/mol

b) Triple Point

Temperature: -70 deg. F

Pressure: 75 psia

c) Normal Boiling Point(14.7 psi)

Temperature: -109.3 deg. F

Latent Heat of Vaporization: 245.5 BTU/lb

d) Other Gas Properties

Gas density (1.013 bar at sublimation point): 2.814 kg/m³

Gas density (1.013 bar and 15 °C (59 °F)): 1.87 kg/m³

Compressibility Factor (Z) (1.013 bar and 15 °C (59 °F)): 0.9942

Specific gravity (air = 1) (1.013 bar and 21 °C (70 °F)): 1.521

Specific volume (1.013 bar and 21 °C (70 °F)): 0.547 m³/kg

Heat capacity at constant pressure (Cp) (1.013 bar and 25 °C (77 °F)): 0.037 kJ/ (mol.K)

Heat capacity at constant volume (Cv) (1.013 bar and 25 °C (77 °F)): 0.028 kJ/ (mol.K)

Ratio of specific heats (γ :Cp/Cv) (1.013 bar and 25 °C (77 °F)) : 1.293759

Viscosity (1.013 bar and 0 °C (32 °F)): 0.0001372 Poise

Thermal conductivity (1.013 bar and 0 °C (32 °F)): 14.65 mW/ (m.K)

Liquid Phase Properties

Liquid density (at -20 °C (or -4 °F) and 19.7 bar): 1032 kg/m³

Liquid/gas equivalent (1.013 bar and 15 °C (per kg of solid)): 845 vol/ vol

Boiling point (Sublimation): -78.5 °C

Latent heat of vaporization (1.013 bar at boiling point): 571.08 kJ/kg

Vapor pressure (at 20 °C or 68 °F): 58.5 bar

APPENDIX B

SPREADSHEET AND VB CODE EXAMPLE

VB Code to calculate Z factor

Public Function zfactor(p, t)

R = 8.314

Tc = 304

Pc = 7.4

molwt = 44

Tr = t / Tc

Pr = p / Pc

Omega = 0.22491

Pi = 3.14159267

m = 0.37464 + 1.54226 * Omega - 0.26992 * Omega ^ 2

alpha = (1 + m * (1 - (Tr ^ 0.5))) ^ 2

A = (0.4572355289 * (R ^ 2) * (Tc ^ 2)) / Pc

aalpha = A * alpha

B = 0.0777960739 * R * Tc / Pc

x = A * alpha * p / ((R * t) ^ 2)

Y = (B * p) / (R * t)

a2 = -(1 - Y)

a1 = x - 3 * (Y ^ 2) - 2 * Y

a0 = -(x * Y - (Y ^ 2) - (Y ^ 3))

$$p1 = ((3 * (a1)) - ((a2) ^ 2)) / 3$$

$$'q1 = (2 * ((a2) ^ 3) - 9 * a2 * a1 + 27 * a0) / 27$$

$$q1 = ((2 * (a2 ^ 3)) - (9 * a2 * a1) + (27 * a0)) / 27$$

$$rn = (((q1) ^ 2) / 4) + ((p1) ^ 3) / 27$$

If rn > 0 Then

'one real root

$$g1 = (-q1 / 2) + (rn ^ 0.5)$$

If g1 > 0 Then

$$pnew = Abs((-q1 / 2) + (rn ^ 0.5)) ^ (1 / 3)$$

Else

$$pnew = -1 * Abs((-q1 / 2) + (rn ^ 0.5)) ^ (1 / 3)$$

End If

$$term1 = (-1 * (q1)) / 2$$

$$term3 = (rn) ^ 0.5$$

$$qnew1 = (term1 - term3)$$

If qnew1 < 0 Then

$$qnew2 = -1 * Abs(qnew1) ^ (1 / 3)$$

Else

$$qnew2 = (qnew1) ^ (1 / 3)$$

End If

$$'qnew = ((-q1) / 2) - (rn ^ 0.5) ^ (1 / 3)$$

$$root = pnew + qnew2$$

$$root11 = root - (a2 / 3)$$

```

zo = root11
Else
'three unequal real roots
mnew = 2 * ((-p1 / 3) ^ 0.5)
theta = (3 * q1) / (p1 * mnew)
theta1 = WorksheetFunction.Acos(theta)
'theta1 = Acos(theta)
theta2 = theta1 / 3
root1 = mnew * Cos(theta2)
root2 = mnew * Cos(theta2 + 4 * Pi / 3)
root3 = mnew * Cos(theta2 + 2 * Pi / 3)
root11 = root1 - (a2 / 3)
root22 = root2 - (a2 / 3)
root33 = root3 - (a2 / 3)
If 217 < t < 400 And 0.52 < p < 7.4 Then
zo = root11
Else
zo = root33
End If
End If
cfactor = zo
zfactor = zo
End Function

```

Table 3. Spreadsheet Output for Calculations on the Annulus Side

n		TD		Choke	Surface		
20		14364 ft		Pressure	Temp		
				100 psi	60 F		
Depth (feet)	Pressure (psi)	Pressure (MPa)	Temp (deg.F)	Temp (K)	Density ppg	Density lb/cu.ft	Viscosity cP
0	100	0.68947	60	288.7056	0.110132	0.823897	0.014409
718.2	115.9455	0.79941	71.41938	295.0497	0.12543	0.938341	0.014736
1436.4	131.1482	0.904227	82.83876	301.3938	0.139297	1.042078	0.015061
2154.6	145.9221	1.006089	94.25814	307.7379	0.152132	1.138102	0.015384
2872.8	160.4487	1.106246	105.6775	314.082	0.164175	1.228191	0.015706
3591	174.8428	1.205489	117.0969	320.4261	0.175579	1.313507	0.016025
4309.2	189.1819	1.304353	128.5163	326.7702	0.186454	1.394861	0.016343
5027.4	203.5205	1.403213	139.9357	333.1143	0.196878	1.472843	0.016658
5745.6	217.8983	1.502343	151.355	339.4584	0.206911	1.547902	0.016972
6463.8	232.3449	1.601948	162.7744	345.8025	0.2166	1.620388	0.017284
7182	246.8829	1.702184	174.1938	352.1466	0.225983	1.690582	0.017595
7900.2	261.53	1.803171	185.6132	358.4907	0.23509	1.758712	0.017903
8618.4	276.2997	1.905004	197.0326	364.8348	0.243947	1.824967	0.01821
9336.6	291.2031	2.007758	208.4519	371.1789	0.252574	1.889509	0.018515
10054.8	306.2486	2.111492	219.8713	377.523	0.260991	1.952473	0.018818
10773	321.4433	2.216255	231.2907	383.8671	0.269212	2.013977	0.019119
11491.2	336.7927	2.322085	242.7101	390.2112	0.277252	2.074123	0.019419
12209.4	352.3013	2.429012	254.1295	396.5553	0.285122	2.133001	0.019717
12927.6	367.9727	2.537061	265.5488	402.8994	0.292834	2.190692	0.020013
13645.8	383.8097	2.646253	276.9682	409.2435	0.300396	2.247266	0.020307
14364	399.8146	2.756602	288.3876	415.5876	0.307818	2.302786	0.0206

APPENDIX C

HEAT TRANSFER MODEL BASED ON THE WORK OF HOLMES AND SWIFT [18]

The model is a solution of the steady-state equation for the heat transfer between the fluids in the annulus and the fluids in the drill pipe. This is combined with an approximate equation for the transient heat transfer between the fluid in the annulus and in the formation. The approximate method may be adequate since the total heat transfer between the two fluids is much greater than that between the annulus fluid and the formation. The low heat transfer between the annulus fluid and the formation is a result of the relatively low thermal conductivity of the formation.

Temperature values are calculated as a function of depth, circulation rate, CO₂ properties, reservoir properties and borehole geometry. The temperature of drilling fluid inside the drill pipe is given as,

$$T_p = K_1 e^{C_1 x} + K_2 e^{C_2 x} + Gx + T_s - GA_3 \quad (C1)$$

and temperature in the annulus is given as

$$T_a = K_1 C_3 e^{C_1 x} + K_2 C_4 e^{C_2 x} + Gx + T_s \quad (C2)$$

where,

$$C_1 = (B_3 / 2A_3)(1 + (1 + 4/B)^{0.5}) \quad (C3)$$

$$C_2 = (B_3 / 2A_3)(1 - (1 + 4/B)^{0.5}) \quad (C4)$$

$$C_3 = 1 + B/2(1 + (1 + 4/B)^{0.5}) \quad (C5)$$

$$C_4 = 1 + B/2(1 - (1 + 4/B)^{0.5}) \quad (C6)$$

$$A_3 = mc_p / 2\pi r_p h_p \quad (C7)$$

$$B_3 = rU / r_p h_p \quad (C8)$$

Forcing the boundary condition that annular and drillpipe fluid temperatures are equal at the bottom of the well gives,

Boundary Condition 1 at $x=0$; $T_p = T_{pi}$

Boundary Condition 2 at $x=H$; $T_{Hp} = T_{Ha}$

Using boundary condition 1 in equation 19 gives

$$K_1 = T_{pi} - K_2 - T_s + GA_3 \quad (C9)$$

Using boundary condition 2 gives

$$K_1 e^{C_1 H} + K_2 e^{C_2 H} - GA_3 = K_1 C_3 e^{C_1 H} + K_2 C_4 e^{C_2 H} \quad (C10)$$

Substituting the value of K_1 from equation 27 in equation 28 gives

$$K_2 = \frac{GA_3 - (T_{pi} - T_s + GA_3) e^{C_1 H} (1 - C_3)}{e^{C_2 H} (1 - C_4) - e^{C_1 H} (1 - C_3)} \quad (C11)$$

where

x = depth, ft,

H = total depth of the well, ft,

c_p = heat capacity of the drilling fluid, BTU/ (lbm- °F)

G = geothermal gradient, °F /ft

T_s = temperature of earth's surface, °F

T_{pi} = inlet temperature of mud in drillpipe, °F

r = radius of well, ft

r_p = radius of drillpipe, ft

m = mass flow rate, lbm/hour

U = overall heat transfer coefficient across wellbore face, BTU/ (sq.ft- °F -hour)

h_p = overall heat transfer coefficient across drillpipe, BTU/ (sq.ft- °F -hour)

This is an approximate method as average properties are considered for heat transfer coefficients and further work using a finite difference approach is recommended. The resulting temperature profile could be illustrated by Figure 4.8. Liquid CO₂ gains heat as it enters the tubing. After exiting the nozzles, it follows the geothermal temperature until, closer to the surface, considerable heat exchange between cold CO₂ in the tubing and the returning CO₂ leads to a drop in its temperature. The Joule-Thompson effect occurs during expansion of SCCO₂ through the nozzles. The NIST data tables [27] indicate that the Joule Thompson coefficient for the CO₂ system is 0.0012 °F/psi, which corresponds to a temperature drop of 6 °F across the nozzles.

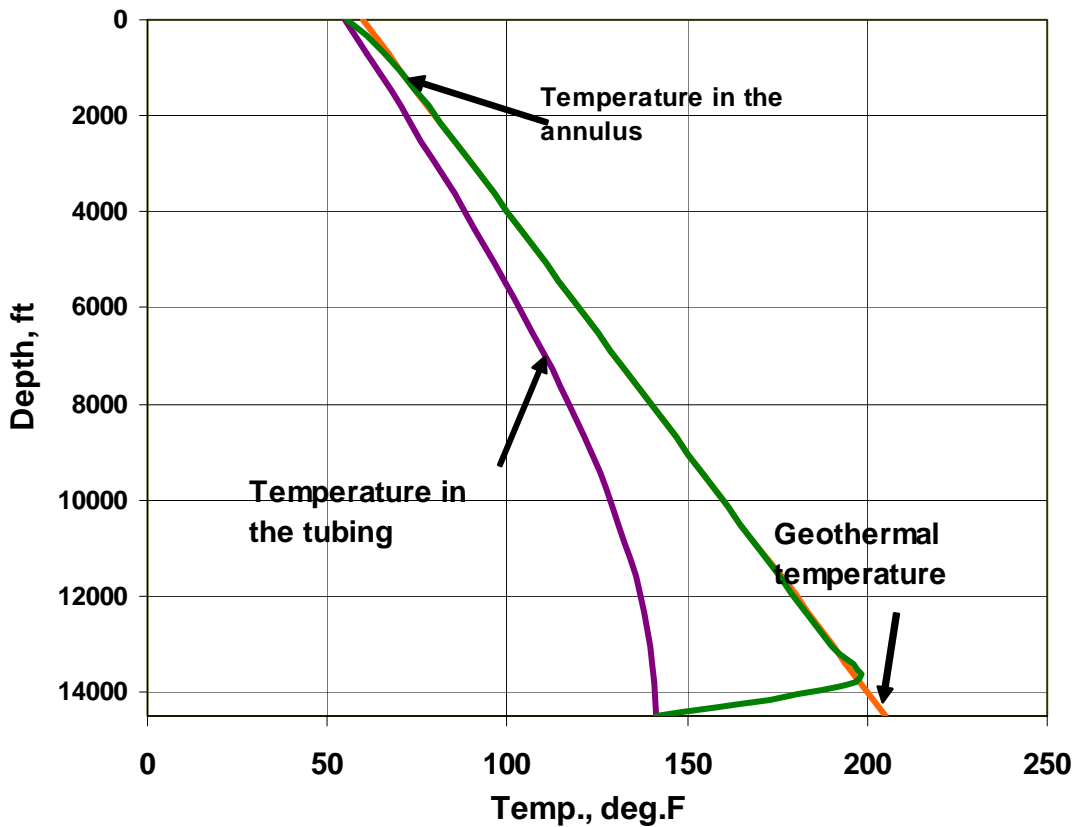


Figure C1. Temperature Profile of CO₂ in the Tubing and Annulus

VITA

Anamika Gupta earned the degree of Bachelor of Engineering in Chemical Engineering in May 2003 from Mumbai University Institute of Chemical Technology, India. She spent the Fall 2003 semester at the University of Missouri, Rolla, before continuing her Master's program in the Department of Petroleum Engineering at Louisiana State University. She is currently doing an internship with Blade Energy Partners, Dallas. Blade offers engineering expertise in underbalanced drilling, deepwater drilling and critical well design.